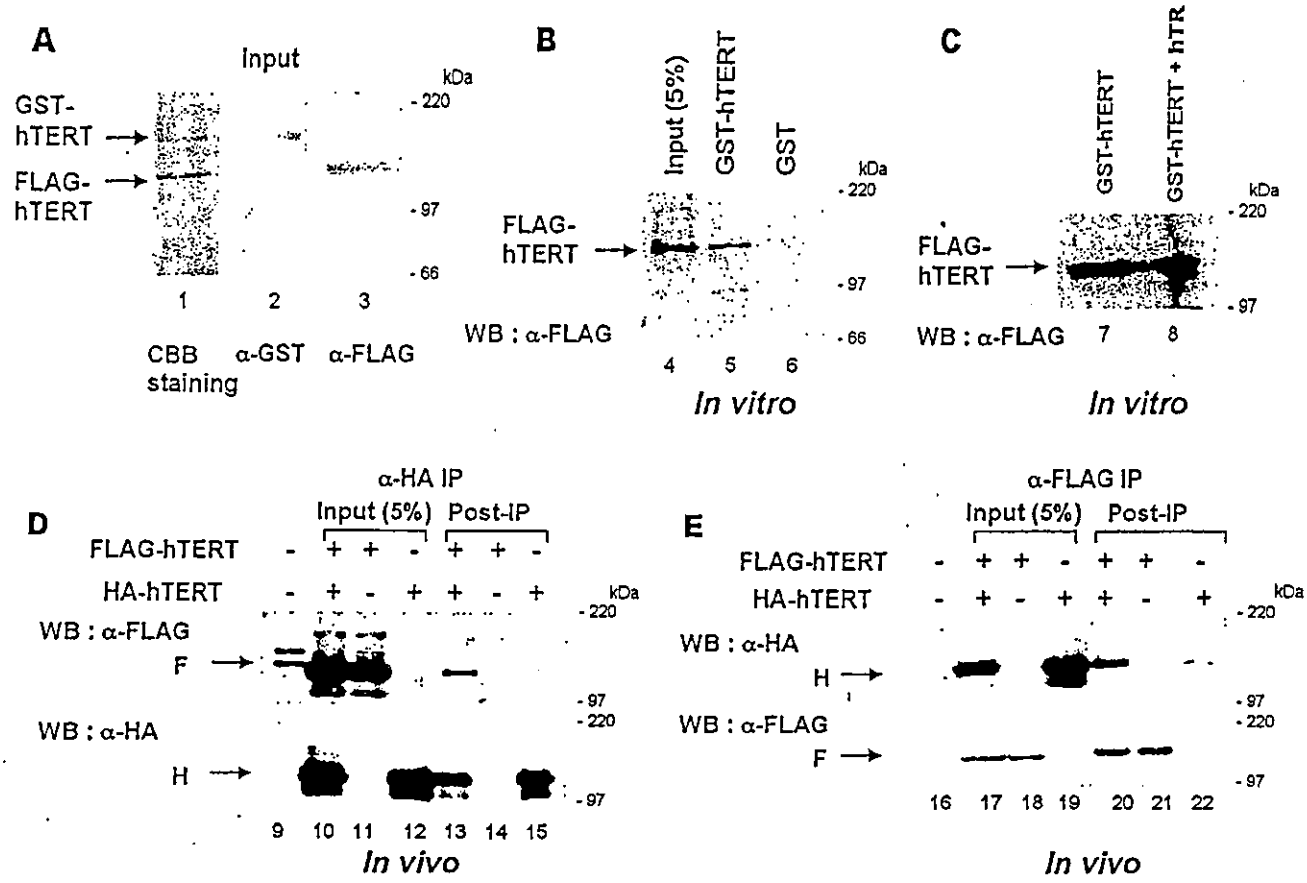

FIG. 1. **Homomeric interaction of hTERT *in vitro* and *in vivo*.** *A* and *B*, FLAG-tagged hTERT and GST-fused hTERT were expressed in High5 cells infected with recombinant baculoviruses and partially purified (*lanes 1–3*). The faster migrating bands in *lane 2* were degraded form of GST-fused hTERT. GST-fused hTERT or GST (expressed in *E. coli*) was incubated on ice with FLAG-tagged hTERT. The mixtures were pulled down by glutathione-Sepharose, then protein bound to the beads was fractionated by 8% SDS-PAGE and subjected to Western blot analysis using anti-FLAG M2 antibody (*lanes 5* and *6*). *C*) GST-fused and FLAG-tagged hTERT proteins were incubated on ice either without (*lane 7*) or with (*lane 8*) purified hTR. The mixtures were subjected to GST pull-down assay, and then bound proteins were detected by Western blot analysis using anti-FLAG M2 antibody. *D* and *E*, HA-tagged hTERT (*H*) and/or FLAG-tagged hTERT (*F*) were co-transfected into COS-1 cells. Cell extracts were immunoprecipitated with anti-HA (*panel D*) or anti-FLAG antibody (*panel E*). The bound proteins were separated by 8% SDS-PAGE, and then subjected to Western blot analysis using anti-HA or anti-FLAG M2 antibody.

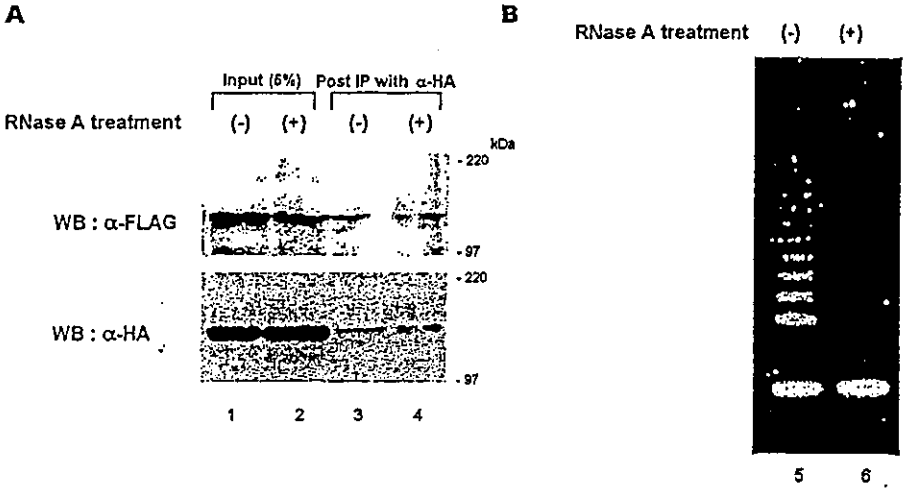

FIG. 2. **The effect of RNase treatment on the homomeric interaction of hTERT.** *A*, HA-tagged hTERT and FLAG-tagged hTERT were co-transfected into COS-1 cells. Cell extracts were treated with 100 μg of RNase A at 30 °C for 15 min, and then immunoprecipitated with anti-HA antibody. The bound proteins were separated by 8% SDS-PAGE and then subjected to Western blot analysis with anti-FLAG M2 or anti-HA antibody. *B*, the telomerase activity of the cell extracts with/without RNase A treatment was measured by TRAP assay.

the putative hTR-binding region (Fig. 3*A*, *lanes 3*, *4*, *7*, and *8*), the carboxyl-terminal region harboring motif E, and the putative thumb domain (Fig. 3*A*, *lanes 1*, *2*, *5*, and *6*), were constructed and the recombinant truncated proteins were purified from insect cells to examine the ability of these proteins to bind GST-hTERT by GST pull-down assay. Three constructs, CF1, NF1, and NF2, bound the wild-type GST-hTERT (Fig. 3*B*, *lanes 11*, *19*, and *23*), whereas CF2 had no binding ability *in vitro* (Fig. 3*B*, *lane 15*). These results indicate that at least the amino- and carboxyl-terminal regions can bind the wild-type hTERT *in vitro*. We then examined the binding abilities of the two regions *in vivo* using truncated versions of FLAG-hTERT in the presence of HA-hTERT in COS-1 cells (Fig. 4*A*, *lanes 2–11*), as well as the ability of the expressed FLAG-hTERT

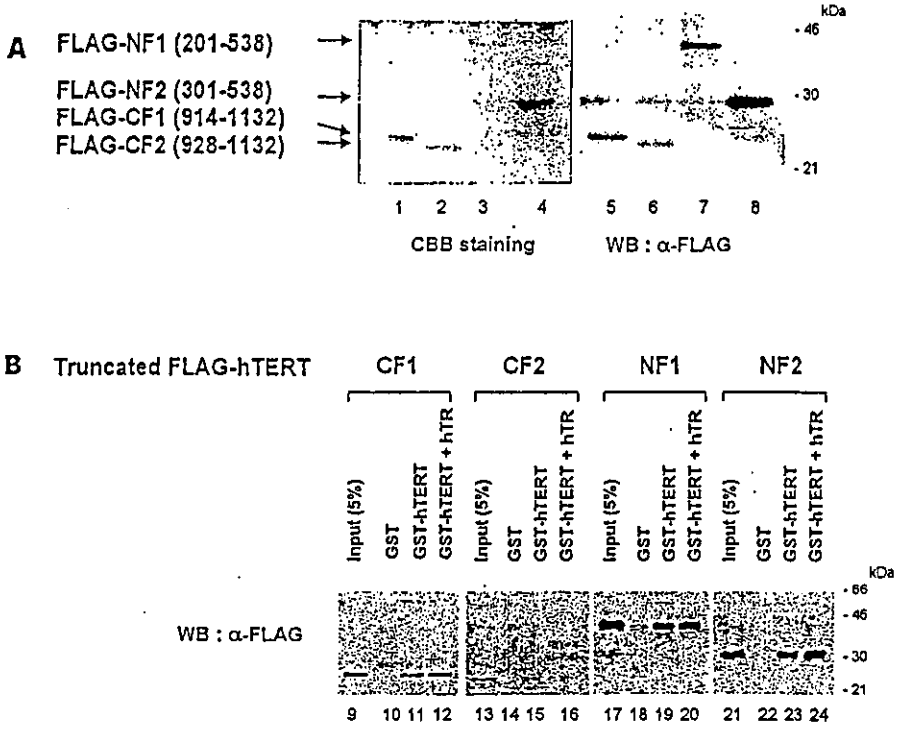

FIG. 3. Two regions can bind the wild-type hTERT *in vitro*. *A*, truncated forms of FLAG-tagged hTERT were expressed in insect cells, partially purified as described under "Experimental Procedures," then analyzed by 12% SDS-PAGE and visualized by Coomassie Brilliant Blue staining (*lanes 1–4*) or subjected to Western blot analysis with anti-FLAG M2 antibody (*lanes 5–8*). Truncated proteins: *lanes 1* and *5*, CF1; *2* and *6*, CF2; *3* and *7*, NF1; *4* and *8*, NF2. *B*, results of GST pull-down assay to evaluate for interaction of partially purified truncated FLAG-tagged hTERT with the wild-type GST-fused hTERT (*lanes 9–12*, interaction with FLAG-CF1; *lanes 13–16*, interaction with FLAG-CF2; *lanes 17–20*, interaction with FLAG-NF1; *lanes 21–24*, interaction with FLAG-NF2). GST-hTERT or GST, immobilized on glutathione beads, was incubated with each partially purified truncated FLAG-hTERT. Bound proteins were fractionated by 12% SDS-PAGE then subjected to Western blot analysis with anti-FLAG M2 antibody.

proteins to HA-hTERT by immunoprecipitation with anti-HA antibody. CF2 and PF did not bind the wild-type hTERT (Fig. 4*A*, *lanes 19* and *22*), whereas the other truncated constructs did (Fig. 4*A*, *lanes 14–18*, *20*, and *21*). Under our experimental conditions, the expression levels of the truncated constructs of FLAG-hTERT proteins differed from those of HA-hTERT proteins. These mapping results *in vivo* and *in vitro* were consistent, indicating that the two independent regions are involved in the homomeric interaction. These two regions are located outside motifs T to D.

The Amino- and Carboxyl-terminal Regions of hTERTs Interact in Vivo—The interactions between the two regions of hTERT and the wild-type hTERT raised two possibilities. The truncated regions may only bind to the wild-type hTERT as a partner, or they may interact with various forms of hTERT. We therefore examined whether these two binding regions interact with each other. Truncated forms of FLAG-hTERT and HA-hTERT were transiently co-expressed in COS-1 cells (Fig. 5*A*, *lanes 1–5* and *11–15*), then co-immunoprecipitated with anti-HA antibody. CF1, aa 914–1132, could bind NF2, aa 301–534, indicating that the truncated amino- and carboxyl-terminal regions interact with each other (Fig. 5*A*, *lane 9*). CF2, aa 928–1132, did not bind to any of the truncated proteins. These results strongly suggest that the amino acid sequence, aa 914–927 including motif E, is critical for the binding. Fig. 5 shows no interaction between the differently tagged amino- or carboxyl-terminal regions (Fig. 5*A*, *lanes 6*, *7*, *16*, and *17*; other data not shown). Thus, the homomeric interaction does not require the wild-type hTERT but does require the amino- and carboxyl-terminal regions. The oligomeric interaction of hTERT proteins may proceed in a head to tail fashion, because the amino- and carboxyl-terminal regions bound each other but not the homologous regions. Under these conditions, NF1, aa 201–534, bound weakly to CF1 compared with NF2 (Fig. 5*A*, *lane 8*). The discrepancy may be due to the limitations of using truncation mutants the structural integrity of which may be disrupted.

hTERT-D712A-V713I and Two Truncation Mutants, CF1 and NF2, Partially Inhibited the Telomerase Activity—To estimate the functional relevance of oligomerization of hTERT for telomerase activity in mammalian cells, finite normal human fibroblasts, TIG-3 cells, were transfected with HA-tagged wild-type hTERT in combination with inactive substituted mutation of hTERT-D712A-V713I at the VDV sequence, which is critical for substrate binding, or several truncated versions of hTERT. Using the lysate of these transfected cells, telomerase activity was measured by TRAP assay and TRAP ELISA. The telomerase activity of the wild-type hTERT was clearly inhibited by hTERT-D712A-V713I in TIG-3 cells compared with that of the wild-type hTERT alone in the TRAP assay (Fig. 6*B*, *lanes 7* and *11*) and TRAP ELISA (Fig. 6*C*). In the TRAP ELISA, the telomerase activity of the wild-type hTERT in TIG-3 cells was partially reduced in combination with hTERT-CF1 or hTERT-NF2, which could bind the wild-type, compared with that in combination with vector or CF2, which could not (Fig. 6*C*). In the TRAP assay, these differences were not clear among the presence of different mutant hTERTs (Fig. 6*B*, *lanes 7–10*). However, in TRAP ELISA experiments, telomerase activity of the wild-type hTERT was inhibited by the truncated mutants in a dose-dependent manner (Fig. 6*D*). This result strongly suggests that the truncation mutants, which can bind to the wild-type hTERT, have a negative effect on telomerase activity.

DISCUSSION

TERT is a unique enzyme among a family of nucleic acid-dependent polymerases harboring a fingers, palm, and thumb substructure, because it forms a tight complex with template RNA for the activity (2, 10, 24). Its long amino- and carboxyl-terminal parts outside of the fingers and palm (aa 525–928) might retain TERT-specific functions (11, 22, 25–28), because these parts are somewhat conserved only among TERTs (9–11). We previously reported that hTERT and hTR are the minimum components required for telomerase activity when telomerase is reconstituted *in vitro* with two purified components (4). During this study we found that the catalytic activity of the purified hTERT was not detectable when concentrations of hTERT were low in the assay reaction (data not shown). This concentration dependence of hTERT reminded us of the template switching of telomerase previously reported in *S. cerevi-*

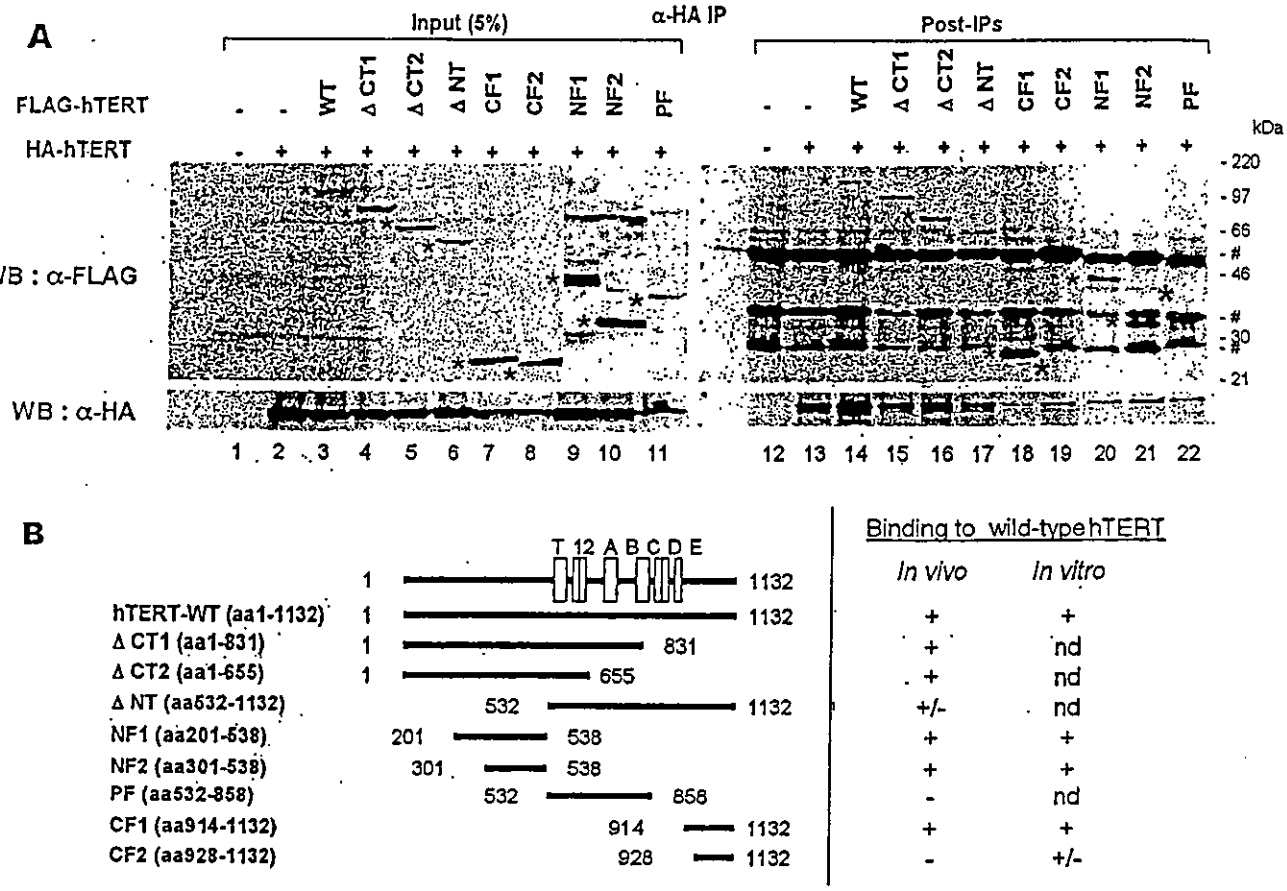

FIG. 4. **Two regions can bind the wild-type hTERT *in vivo*.** *A*, HA-tagged wild-type hTERT and the wild-type or truncated FLAG-tagged hTERT were transiently co-expressed in COS-1 cells. Cell extracts were immunoprecipitated with anti-HA antibody immobilized on protein A-Sepharose. Bound proteins were separated by 12% SDS-PAGE and subjected to Western blot analysis with anti-FLAG M2 (*upper panels*) or anti-HA antibodies (*lower panels*). Truncated proteins: *lanes 2–11* and *13–22*, HA-hTERT; *3* and *14*, the wild-type FLAG-hTERT; *4* and *15*, FLAG-ΔCT1; *5* and *16*, FLAG-ΔCT2; *6* and *17*, FLAG-ΔNT; *7* and *18*, FLAG-CF1; *8* and *19*, FLAG-CF2; *9* and *20*, FLAG-NF1; *10* and *21*, FLAG-NF2; *11* and *22*, FLAG-PF. *Asterisks* indicate specific bands for each the wild-type or truncated FLAG-hTERT protein. #, immunoglobulin chains. *B*, mapping of oligomeric interaction of hTERT by truncation analysis. hTERT and truncations were drawn schematically. The motifs conserved within various reverse transcriptases are represented by *boxes 1*, *2*, *A*, *B*, *C*, *D*, and *E* (22). The motif found specifically within TERT proteins is represented by *box T* (10).

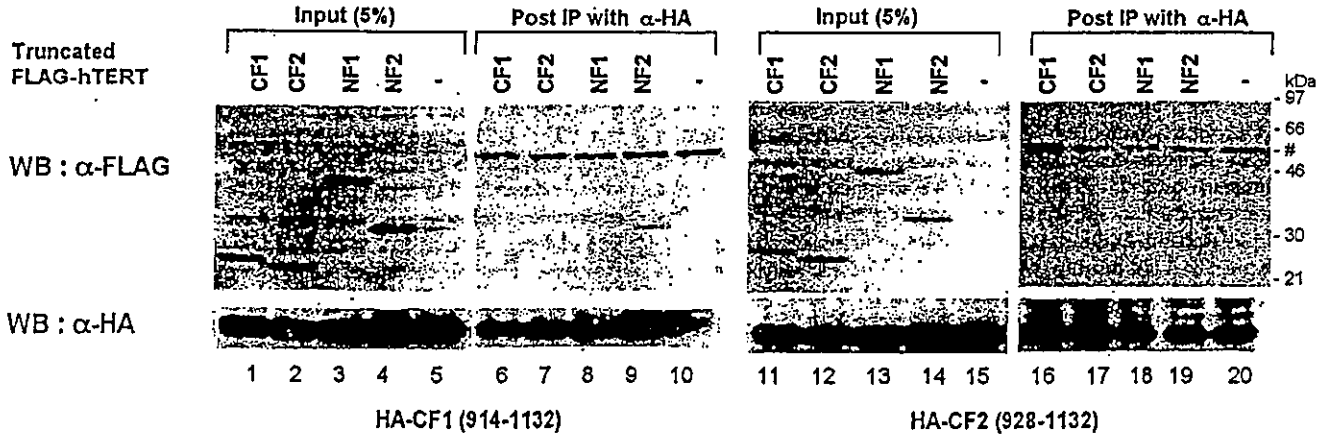

FIG. 5. **Two binding regions interact *in vivo*.** HA-tagged truncated hTERT and truncated FLAG-tagged hTERT were co-expressed in COS-1 cells by transient transfection. Cell extracts were immunoprecipitated with anti-HA antibody immobilized on protein A-Sepharose. Bound proteins were fractionated by 12% SDS-PAGE and then subjected to Western blot analysis with anti-FLAG M2 (*upper panels*) or anti-HA antibodies (*lower panels*). Truncated proteins: *lanes 1–10*, HA-CF1; *11–20*, HA-CF2; *1*, *6*, *11*, and *16*, FLAG-CF1; *2*, *7*, *12*, and *17*, FLAG-CF2; *3*, *8*, *13*, and *18*, FLAG-NF1; *4*, *9*, *14*, and *19*, FLAG-NF2. #, immunoglobulin chains.

siae (17) and the oligomeric interactions of poliovirus (15) and hepatitis C virus RdRPs (29). Two groups recently reported the oligomeric role of telomerase using the different methods (18, 19). However, it was not clear whether TERT forms multimer intrinsically or with help of template RNA. Here we show that the homomeric interaction of hTERT *in vitro* with partially purified differently tagged-hTERTs. Human TR seems to have no effect on the structural oligomerization of hTERT (Fig. 1*C*), and RNase treatment did not affect the homomeric interaction *in vivo* (Fig. 2*A*) and *in vitro* (data not shown). These results

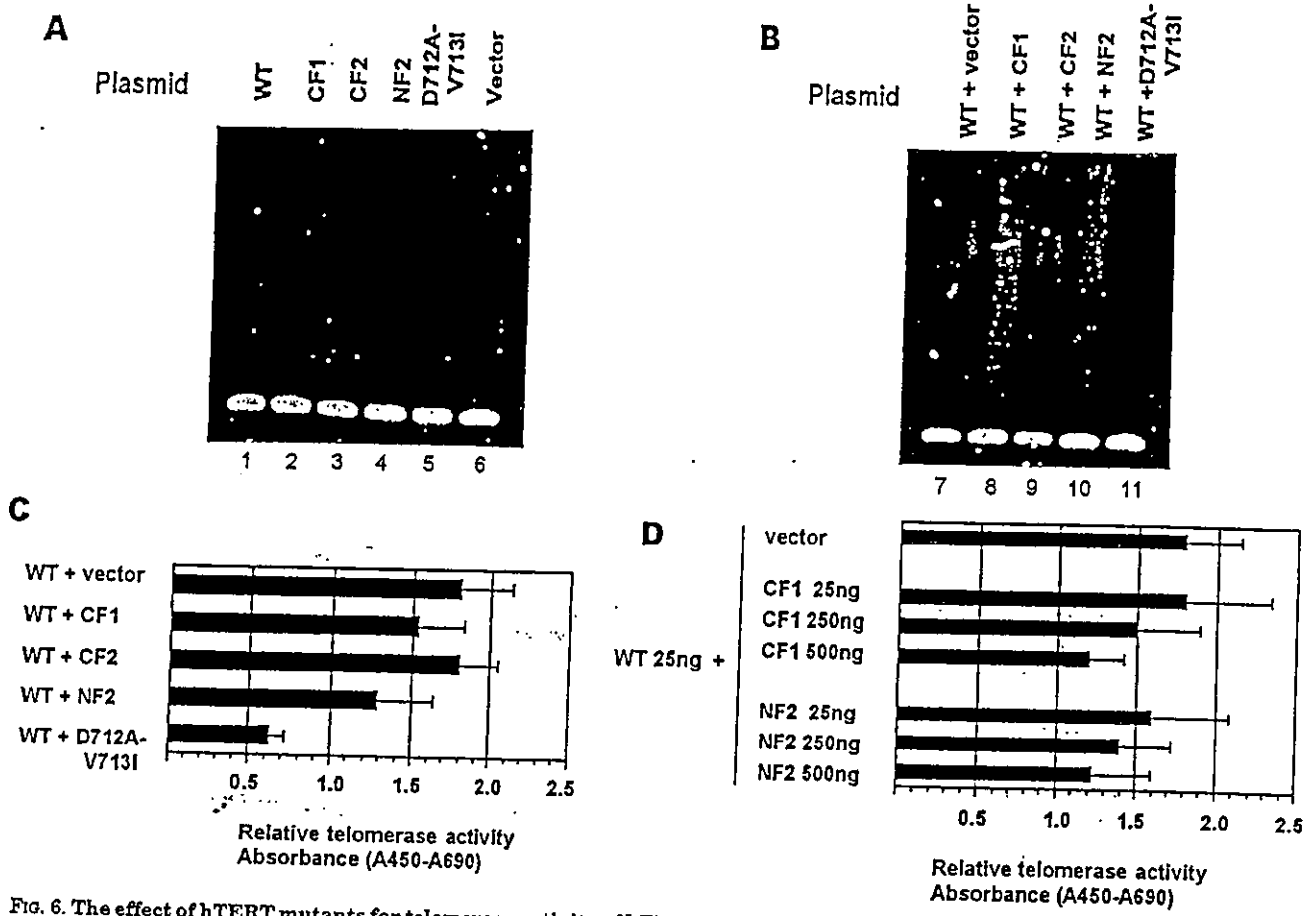

FIG. 6. **The effect of hTERT mutants for telomerase activity of hTERT *in vivo*.** *A*, lysate (100 μg) prepared from the TIG-3 cells transiently transfected with the wild-type hTERT, hTERT-CF1, hTERT-CF2, hTERT-NF2, hTERT-D712A-V713I, or vector was assayed for telomerase activity by TRAP assay. *B* and *C*, cell lysate, 100 μg (*B*) or 1 μg (*C*), prepared from the TIG-3 cells transiently co-transfected both with 25 ng of the wild-type hTERT and with 500 ng of vector, hTERT-CF1, hTERT-CF2, hTERT-NF2, and hTERT-D712A-V713I were assayed for telomerase activity by TRAP assay (*B*) and TRAP ELISA (*C*). *D*, lysate (100 μg) prepared from the TIG-3 cells transiently co-transfected both with 25 ng of the wild-type hTERT and with increasing amounts of hTERT-CF1 or hTERT-NF2 were assayed for telomerase activity by TRAP ELISA. Data are shown as the mean ± S.D.

indicate that hTERT has an intrinsic ability to oligomerize in the absence of intact hTR.

Two separate regions of hTERT (aa 301–538 and aa 914–1132) can be mapped to bind the wild-type hTERT *in vitro* and *in vivo*. This result may be consistent with a previous report (25) in which some combinations of two different truncated hTERT mutants defective in telomerase activity reconstituted telomerase activity. Two regions we mapped are outside the fingers and palm substructure covering motifs T to D. The amino-terminal fragment, aa 301–538, overlaps the region important for hTR binding (25, 26, 30). The carboxyl-terminal fragment, aa 914–1132, includes motif E and a putative thumb. The two separate regions can bind each other, but no homologous interaction of aa 301–538 or aa 914–1132 was detected (Fig. 4*A* and data not shown). The result seems to support a model that the homomeric interaction of hTERT occurs in a "head to tail" fashion. Our result cannot explain the previous result that the amino-terminal region (aa 1–300) and some truncated mutants (such as aa 301–1132) reconstituted telomerase activity (25). The region (aa 1–300) critical for telomerase activity (25, 26) may be not essential for the oligomerization but essential to interact with one or more critical factors such as hTR-binding proteins or Hsp90, which is recruited to telomerase by hTR or hTERT.

Functional oligomeric formations of telomerase have been proposed since two functional template RNAs in the telomerase complex having two active sites were found in *S. cerevisiae* and in humans (17, 18). In our experiments, the substituted mutant hTERT-D712A-V713I, bound to the wild-type hTERT *in vivo* and *in vitro* (data not shown) and inhibited its telomerase activity (Fig. 6), suggesting that oligomeric formation of the wild-type and the mutant hTERTs is the reason of the inhibition. The D712A or D712A-V713I mutants at the VDV sequence, which is critical for substrate binding, have been previously described as dominant negative mutants that eliminate endogenous telomerase activity and cause telomere shortening and cell senescence due to lack of telomerase activity (23, 31). However, the inhibitory effect of the mutant on the wild-type hTERT was not severe when transiently co-expressed in the telomerase-negative cells even if the amount of plasmid of the mutant was more than 10 times higher than the wild-hTERT (Fig. 6). The result seems to be consistent with the previous report by Beattie *et al.* (25) who observed a partial restoration of telomerase activity in the presence of hTERT-D712A and the truncated hTERTs harboring the intact pocket for active center but missing the amino-terminal region. These results suggest that the mutants defective in substrate binding (D712A or D712A-V713I) are not dominant negative enzymatically when these mutants oligomerized with the wild-type hTERT, although reconstituted telomerase activity of oligomers consisting of the wild-type and D712A or D712A-V713I hTERTs seems to be much weaker than that of the wild-type oligomer (Fig. 6) (25). The apparent dominant negative phenotype of D712A or D712A-V713I in the previous reports may be explained by a

huge difference in expression levels between endogenous hTERT and the ectopically expressed mutant hTERT, which may squelch out one or more critical factors for telomerase activity.

We expected that the truncated mutants, which have the hTERT-binding regions, would exhibit strong inhibitory effects on the wild-type hTERT by competing oligomerization of the wild-type hTERT. Rather weak inhibitory effects of the amino-terminal and the carboxyl-terminal binding regions may be due to weaker binding abilities to the wild-type hTERT or inefficient recruitment of the proteins to the wild-type hTERT.

Telomere maintenance is essential to the replicative potential of malignant cells, and inhibition of telomerase leads to telomere shorting and cessation of unrestrained proliferation (9, 10, 23, 31–33). The intrinsic property of hTERT to oligomerize may be an additional target to design specific inhibitors of telomerase. This strategy has been applied to HIV reverse transcriptase (14, 34–36).

Acknowledgments—We are grateful to W. Hahn, L. Harrington, N. Hayashi, M. Hirano, and W. Qin for encouraging discussions, and to F. Momoshima, M. Yasukawa, and K. Kuwabara for technical assistance.

REFERENCES

1. McEachern, M. J., Krauskopf, A., and Blackburn, E. H. (2000) *Annu. Rev. Genet.* 34, 331–358
2. Nugent, C. I., and Lundblad, V. (1998) *Genes Dev.* 12, 1073–1085
3. Bodnar, A. G., Ouellette, M., Frolkis, M., Holt, S. E., Chiu, C. P., Morin, G. B., Harley, C. B., Shay, J. W., Lichtsteiner, S., and Wright, W. E. (1998) *Science* 279, 349–352
4. Masutomi, K., Kaneko, S., Hayashi, H., Yamashita, T., Shirota, Y., Kobayashi, K., and Murakami, S. (2000) *J. Biol. Chem.* 275, 22568–22573
5. Nakayama, J., Tahara, H., Tahara, E., Saito, M., Ito, K., Nakamura, H., Nakanishi, T., Tahara, E., Ide, T., and Ishikawa, F. (1998) *Nat. Genet.* 18, 65–68
6. Kohlstaedt, L. A., Wang, J., Friedman, J. M., Rice, P. A., and Steitz, T. A. (1992) *Science* 256, 1783–1790
7. Sousa, R. (1996) *Trends Biochem. Sci.* 21, 186–190
8. Bressanelli, S., Tomei, L., Roussel, A., Incitti, I., Vitale, R. L., Mathieu, M., De Francesco, R., and Rey, F. A. (1999) *Proc. Natl. Acad. Sci. U. S. A.* 96, 13034–13039
9. Meyerson, M., Counter, C. M., Eaton, E. N., Ellisen, L. W., Steiner, P., Caddle, S. D., Ziaugra, L., Beijersbergen, R. L., Davidoff, M. J., Liu, Q., Bacchetti, S., Haber, D. A., and Weinberg, R. A. (1997) *Cell* 90, 785–795
10. Nakamura, T. M., Morin, G. B., Chapman, K. B., Weinrich, S. L., Andrews, W. H., Lingner, J., Harley, C. B., and Cech, T. R. (1997) *Science* 277, 955–959
11. Xia, J., Peng, Y., Mian, I. S., and Lue, N. F. (2000) *Mol. Cell. Biol.* 20, 5196–5207
12. Muller, B., Restle, T., Weiss, S., Gautel, M., Sczakiel, G., and Goody, R. S. (1989) *J. Biol. Chem.* 264, 13975–13978
13. Restle, T., Muller, B., and Goody, R. S. (1990) *J. Biol. Chem.* 265, 8986–8988
14. Tachedjian, G., Aronson, H. E., and Goff, S. P. (2000) *Proc. Natl. Acad. Sci. U. S. A.* 97, 6334–6339
15. Hobson, S. D., Rosenblum, E. S., Richards, O. C., Richmond, K., Kirkegaard, K., and Schultz, S. C. (2001) *EMBO J.* 20, 1153–1163
16. Qin, W., Luo, H., Nomura, T., Hayashi, N., Yamashita, T., and Murakami, S. (2002) *J. Biol. Chem.* 277, 2132–2137
17. Prescott, J., and Blackburn, E. H. (1997) *Genes Dev.* 11, 2790–2800
18. Wenz, C., Enenkel, B., Amacker, M., Kelleher, C., Damm, K., and Lingner, J. (2001) *EMBO J.* 20, 3526–3534
19. Beattie, T. L., Zhou, W., Robinson, M. O., and Harrington, L. (2001) *Mol. Cell. Biol.* 21, 6151–6160
20. Yamashita, T., Kaneko, S., Shirota, Y., Qin, W., Nomura, T., Kobayashi, K., and Murakami, S. (1998) *J. Biol. Chem.* 273, 15479–15486
21. Lin, Y., Nomura, T., Yamashita, T., Dorjsuren, D., Tang, H., and Murakami, S. (1997) *Cancer Res.* 57, 5137–5142
22. Counter, C. M., Hahn, W. C., Wei, W., Caddle, S. D., Beijersbergen, R. L., Lansdorp, P. M., Sedivy, J. M., and Weinberg, R. A. (1998) *Proc. Natl. Acad. Sci. U. S. A.* 95, 14723–14728
23. Hahn, W. C., Stewart, S. A., Brooks, M. W., York, S. G., Eaton, E., Kurachi, A., Beijersbergen, R. L., Knoll, J. H., Meyerson, M., and Weinberg, R. A. (1999) *Nat. Med.* 5, 1164–1170
24. Xiong, Y., and Eickbush, T. H. (1990) *EMBO J.* 9, 3353–3362
25. Beattie, T. L., Zhou, W., Robinson, M. O., and Harrington, L. (2000) *Mol. Biol. Cell* 11, 3329–3340
26. Armbruster, B., Banik, S. R. S., Guo, C., Smith, C. A., and Counter, M. C. (2001) *Mol. Cell. Biol.* 21, 7775–7786
27. Seimiya, H., Sawada, H., Muramatsu, Y., Shimizu, M., Ohko, K., Yamane, K., and Tsuruo, T. (2000) *EMBO J.* 19, 2652–2661
28. Zhu, J., Wang, H., Bishop, J. M., and Blackburn, E. H. (1999) *Proc. Natl. Acad. Sci. U. S. A.* 96, 3723–3728
29. Qin, W., Yamashita, T., Shirota, Y., Lin, Y., Wei, W., and Murakami, S. (2001) *Hepatology* 33, 728–737
30. Bachand, F., and Autexier, C. (2001) *Mol. Cell. Biol.* 21, 1888–1897
31. Zhang, X., Mar, V., Zhou, W., Harrington, L., and Robinson, M. O. (1999) *Genes Dev.* 15, 2388–2399
32. Kim, N. W., Piatyszek, M. A., Prowse, K. R., Harley, C. B., West, M. D., Ho, P. L., Coviello, G. M., Wright, W. E., Weinrich, S. L., and Shay, J. W. (1994) *Science* 266, 2011–2015
33. Ramakrishnan, S., Eppenberger, U., Mueller, H., Shinkai, Y., and Narayanan, R. (1998) *Cancer Res.* 58, 622–625
34. Harris, D., Lee, R., Misra, H. S., Pandey, P. K., and Pandey, V. N. (1998) *Biochemistry* 37, 5903–5908
35. Divita, G., Restle, T., Goody, R. S., Chermann, J. C., and Baillon, J. G. (1994) *J. Biol. Chem.* 269, 13080–13083
36. Morris, M. C., Robert-Hebmann, V., Chaloin, L., Mery, J., Heitz, F., Devaux, C., Goody, R. S., and Divita, G. (1999) *J. Biol. Chem.* 274, 24941–24946

Establishment of a Highly Efficient Gene Transfer System for Mouse Fetal Hepatic Progenitor Cells

Kentaro Yasuchika,[1] Tetsuro Hirose,[2] Hideaki Fujii,[1] Shoshiro Oe,[1] Koichi Hasegawa,[3] Takahisa Fujikawa,[1] Hisaya Azuma,[1] and Yoshio Yamaoka[1]

Because of a donor shortage problem in liver transplantation, cell transplantation has been anticipated as a useful bridge or substitute therapy, and has necessitated the development of cell sources other than donated organs. Therefore, the use of fetal hepatic progenitor cells (HPCs) is now being focused on. In this study, we intended to establish an efficient *ex vivo* nonviral gene-transfer system using a newly developed isolation and culture system for mouse fetal HPCs. Fetal HPCs, characterized using immunocytochemistry and reverse-transcription polymerase chain reaction (RT-PCR) for lineage markers, were collected from E13.5 Balb/c mice using change in size because of cell aggregation by their homophilic cell-to-cell binding occurring during suspension culture. Optimal conditions for culture and *ex vivo* gene transfection for fetal HPCs were determined by ^{3}H-thymidine incorporation and the expression efficacy of transfected red fluorescent protein (DsRed) gene in different culture media. The optimum timing for gene transfection was also evaluated. To evaluate the *in vivo* expression of the transferred gene, DsRed-transferred fetal HPCs were transplanted into 70% partially hepatectomized allogenic mice. The highest efficacy of DsRed gene transfection into fetal HPCs *in vitro* (45% ± 12.3%) was achieved with culture media, which also enabled the highest ^{3}H-thymidine incorporation, containing the deleted form of hepatocyte growth factor (dHGF) and insulin, and when transfection was performed immediately after isolation. *In vivo* DsRed expression in fetal HPCs was maintained concomitantly with albumin expression even after HPC transplantation. In conclusion, we established a highly efficient *in vitro* gene transfer system for mouse fetal HPCs using a newly developed isolation and culture system. (HEPATOLOGY 2002;36:1488-1497.)

Although orthotopic liver transplantation has been established as one of the therapeutic modalities against severe liver diseases, donor shortage remains one of the main problems and some alternatives are needed. On the other hand, hepatocyte use in cell transplantation[1-4] and bioartificial livers have proved useful in improving liver function adequately enough to extend the waiting time for liver transplantation.[5-11] Moreover, these optimal strategies are anticipated not only for bridge use but also as alternative therapy against some of the severe liver disorders, consequently allowing a partial solution to the donor-shortage problem. However, to establish these optimal strategies as clinical therapies, the development of cell sources other than donated organs is indispensable. From this point of view, we are now focusing on the usage of fetal hepatic progenitor cells (HPCs) for the following reasons. First, HPCs have a significantly higher proliferation ability than adult hepatocytes, which may be an ideal characteristic for a cell source. Second, HPCs also have an advantage in terms of immunologic problems because they are reported to lack the expression of classical MHC class 1 antigen,[12] possibly leading to a reduced immunoreaction in HPC use for cell transplantation as a result of immunologic tolerance.[13-17] In addition to these advantages, if effective gene transfer into fetal HPCs becomes possible, they can theoretically be a useful and convenient

Abbreviations: HPC, hepatic progenitor cell; AFP, α-fetoprotein; FITC, fluorescein isothiocyanate; ALB, albumin; CK19, cytokeratin 19; IgG, immunoglobulin G; dHGF, deleted form of hepatocyte growth factor; FCS, fetal calf serum; EDTA, ethylenediaminetetraacetic acid; DNase, deoxyribonuclease; PBS, phosphate-buffered saline; RT-PCR, reverse-transcription polymerase chain reaction.

From the [1]Department of Gastroenterological Surgery, Kyoto University Graduate School of Medicine; the [2]Department of Regenerative Medicine, Institute for Frontier Medical Sciences; and the [3]Department of Development and Differentiation, Institute for Frontier Medical Sciences, Kyoto University, Kyoto, Japan.

Received January 28, 2002; accepted September 11, 2002.

Supported by Health Sciences Research Grants from the Ministry of Health Labour and Welfare and by grants from the Ministry of Education, Science, Culture, and Sports of Japan (12470256) and the Japan Society for the Promotion of Science (RFTF96I00204).

Address reprint requests to: Kentaro Yasuchika, M.D., Department of Gastroenterological Surgery, Kyoto University Graduate School of Medicine, 54 Shogoin Kawaracho, Sakyo-ku, Kyoto City 606-8507, Japan. E-mail: kent@kuhp.kyoto-u.ac.jp; fax: (81) 75-751-4263.

Copyright © 2002 by the American Association for the Study of Liver Diseases.

0270-9139/02/3606-0025$35.00/0

doi:10.1053/jhep.2002.36951

cell source for chronic liver diseases, including congenital enzyme deficiency.[2,7,18] Nevertheless, there is no evidence showing the possibility of gene transfer into fetal HPCs to date. To realize this possibility, we developed a highly efficient *in vitro* gene transfer system in mouse fetal HPCs in a nonviral fashion using a new isolation method and culture system, and achieved continuous gene expression *in vivo* even after fetal HPC transplantation. Our results are the first evidence indicating the possibility of HPC use as a nonviral vector for cellular gene therapy.

Materials and Methods

Animals. Balb/c mice obtained from SLC (Hamamatsu, Japan) were used. Fetal HPCs were obtained from E13.5 fetuses and were transplanted into 5- to 7-week-old male mice in transplantation experiments. The animals were maintained at a constant temperature of 18°C to 20°C and in a 12-hour-light/12-hour-dark cycle. They were kept according to the Animal Protection Guidelines of Kyoto University.

Reagents and Antibodies. The antibodies used in the immunocytochemistry were as follows. The first antibodies used were goat anti-mouse α-fetoprotein (AFP) polyclonal antibody (Santa Cruz Biotechnology, Inc., Santa Cruz, CA), fluorescein isothiocyanate (FITC)-conjugated goat anti-mouse albumin (ALB) polyclonal antibody (Bethyl Laboratories, Inc., Montgomery, TX), and mouse hybridoma anti-mouse keratin monoclonal antibody (ICN Pharmaceuticals, Inc., Aurora, OH) to detect cytokeratin 19 (CK19). The second antibodies used were biotin-conjugated rabbit anti-goat immunoglobulin G (IgG) (Chemicon International, Inc., Temecula, CA) and biotin-conjugated anti-mouse IgG1 (Santa Cruz Biotechnology, Inc.). A deleted form of hepatocyte growth factor (dHGF)[19-20] added to the culture media was a kind gift from Snow Brand Industry Co., Ltd. (Osaka, Japan). Insulin added to the culture media was obtained from Sigma Chemical Co., Ltd. (St. Louis, MO).

Isolation and Culture of HPC. A pregnant Balb/c mouse at day 13.5 of gestation was killed and underwent cesarean section. Several fetuses (5 to 12) were removed at a time, and their liver tissues were dissected and placed in cold Ca^{2+}-free Hank's balanced salt solution containing 10% fetal calf serum (FCS), 10 mmol/L HEPES, 0.5 mmol/L ethylenediaminetetraacetic acid (EDTA) and 2 units/mL heparin. They were then minced into pieces and incubated at 37°C in digestion medium containing 0.5% collagenase (Life Technologies, Inc., Rockville, MD) and 2 units/mL heparin for 15 minutes. The digested tissues were filtered through a nylon mesh (70-μm pore size) and centrifuged at ×40*g*. The cell viability was estimated by the trypan blue exclusion test. After an additional wash in cold Ca^{2+}-free Hank's balanced salt solution with 0.05% deoxyribonuclease (DNase) I (Sigma Chemical Co., Ltd.), the dissociated cells were suspended in RPMI 1640 supplemented with 1.0×10^2 units/mL penicillin G and 0.2 mg/mL streptomycin, with or without 10% FCS, 10 ng/mL dHGF, or 600 ng/mL insulin. The dissociated cells were inoculated onto Petri dishes (Falcon; Becton Dickinson Labware, Franklin Lakes, NJ) at a density of 5.0×10^5 cells/mL. After 12 hours of incubation, the aggregated cells were collected in 15-mL conical tubes (Falcon; Becton Dickinson Labware) and subjected to gravity sedimentation for 10 minutes. After the supernatant was removed, the sedimented cell aggregates were resuspended in new culture media and then inoculated on type I collagen-coated culture plates (Becton Dickinson Co., Ltd., Lincoln Park, NJ). After an additional day of culture, they adhered to the plates and extended as monolayer colonies. Thereafter, the culture media were changed every 2 days.

Immunocytochemistry. The cells were fixed in 3.3% formalin for 12 minutes at room temperature. Then, endogenous peroxidase activity was blocked with 1% H_2O_2 in methanol for 15 minutes. Also, endogenous avidin and biotin were blocked with an avidin/biotin blocking kit (Vector Laboratories, Inc., Burlingame, CA). Nonspecific binding was blocked with 0.4% bovine serum albumin (Sigma-Aldrich Chemie Co., Ltd., Steinheim, Germany) in 0.1% saponin (Sigma Chemical Co., Ltd.)-phosphate-buffered saline (PBS). Subsequently, they were incubated with the first antibody for 16 hours at 4°C followed by incubation with the biotin-conjugated second antibody for 30 minutes at room temperature. All of the antibodies were diluted to the optimal concentration in 0.1% saponin-PBS for permeability. After reaction with streptavidin-peroxidase complex, a tyramide signal amplification system (NEN Life Science Products, Inc., Boston, MA) with Texas Red (Eugene Co., Ltd., Eugene, OR) was used for the detection of an immunologic reaction against AFP and CK19. ALB was detected as green fluorescence of FITC, which was conjugated to the first antibody. Nuclear counterstain was done with 4′, 6-diamidino-2-phenylindole. The signal was detected using a fluorescent microscope (Axiovert 135, Carl Zeiss Vision Co., Ltd., Hallbergmoos, Germany).

Reverse-Transcription Polymerase Chain Reaction. The character of the isolated cells was evaluated by reverse-transcription polymerase chain reaction (RT-PCR). mRNA was extracted from the cell colonies using a QuickPrep Micro mRNA purification kit (Amersham Pharmacia Biotech UK, Ltd., Buckinghamshire, UK) according to the supplier's recommended protocol. cDNA

Table 1. Primer Sequences Used

AFP	5′-GAAGATGGTGAGCATTGCC-3′	5′-AACAGACTTCCTGGTCCTGG-3′
ALB	5′-CGAGAAGCTTGGAGAATATGG-3′	5′-GTCAGAGCAGAGAAGCATGG-3′
CK19	5′-GTGCCACCATTGACAACTCC-3′	5′-AATCCACCTCCACACTGACC-3′
flk-1	5′-TGACATGCACAGTCTACGCC-3′	5′-ACTGGTGTGAGTGATTCGCC-3′
VE-cadherin	5′-AGGCTGAATACAAGATCGTGG-3	5′-GGTCTGTCTCAATGGTGAAGG-3′
CD34	5′-ACACATCATCTTCTGCTCCG-3′	5′-CTGTGCTATTGGCCAAGACC-3′
desmin	5′-GCTATCAGGACAACATTGCG-3′	5′-GTTGTTGCTGTGTAGCCTCG-3′
CD45	5′-GTGCCTTGTTCAATCTCTTGG-3′	5′-CAGTTAGCATCCTGCTTGCC-3′
β-actin	5′-TCCTATGTGGGTGACGAGGC-3′	5′-TACATGGCTGGGGTGTTGAA-3′

was synthesized using random hexamer primers and an Omniscript RT kit (Qiagen Co., Ltd., Hilden, Germany). PCR was done using HotStarTaq DNA polymerase (Qiagen Co., Ltd.) with specific primer pairs. The primer sequences used are shown in Table 1. The amplified products were not observed in the absence of reverse transcriptase, excluding the possibility of genomic DNA contamination in the starting materials.

^{3}H-Thymidine Incorporation Into Fetal HPC. ^{3}H-Thymidine incorporation into cell clusters of fetal HPCs was investigated to evaluate the optimal growth media composition for fetal HPC culture. One day after the fetal HPC isolates formed cell aggregates, they were inoculated on 96-well culture plates in triplicate and cultured for 3 days with 80 μL of culture media in each well in the presence or absence of 10% FCS, dHGF (10 ng/mL), and insulin (600 ng/mL). Twenty microliters of ^{3}H-thymidine (10 μCi/mL) was added to the culture media for the last 48 hours. The radioactivity of each well was detected using a scintillation counter (Tri-Carb 1900CA, Hewlett-Packard Co., Ltd., Palo Alto, CA) as previously described.[21]

Gene Transfer Into Fetal HPC. pCAGmitoDsRed encoding *Discosoma* sp. red fluorescent protein (DsRed) with a mitochondrial targeting sequence was used in the transfection experiments. The plasmid was transfected into HPCs using Effectene transfection reagent (Qiagen Co., Ltd.) concomitantly with or 6 hours after inoculation of the fetal HPCs on Petri dishes. Transfection efficacy among several transfection reagents was compared in preliminary experiments, and Effectene transfection reagents proved to be the most suitable for the transfection of exogenous genes into mouse fetal HPCs (data not shown). After 8 to 12 hours of incubation, the efficacy of gene expression was evaluated using a fluorescent microscope. Also, the transfection efficiency was evaluated 24 hours after the inoculation of fetal HPCs on type I collagen-coated plates where they formed monolayer colonies. The number of DsRed-expressing cells was counted in 10 different random fields.

Southern Blot Analysis. The DsRed gene was transferred into fetal HPCs under the determined condition after the above experiments. After 4 days of culture, the genomic DNA of gene-transferred HPCs was extracted with a DNA extraction kit (Qiagen Co., Ltd.), which can extract DNA of approximately 30 kb in size and cannot extract the episomal vector plasmid pCAGmitoDsRed (5.6 kb). Similarly, the genomic DNA of HPCs, into which the DsRed gene was not transferred, was extracted as a negative control experiment. The same amounts of these DNA (10 μg) were supplied for digestion by restriction enzyme, *Hind*III, which cut the vector plasmid at one portion. After the digestion, these DNA samples were subjected to electrophoresis in 0.8% agarose gel for 5 hours. Then, they were blotted on a nylon filter (Hybond-N+, Amersham-Pharmacia Biotech UK Limited) and hybridized by DsRed probe, which was constructed from pDsRed-N1 (Clontech Laboratories, Inc., Palo Alto, CA) with *BamH*I-*Not*I digestion and labeled with an Alkaphos DNA Labeling kit (Amersham-Pharmacia Biotech UK Limited) according to the manufacturer's method. The chemiluminescence of alkaline phosphatase representing the integrated DsRed gene was detected using CDP-*Star* detection reagent (Amersham-Pharmacia Biotech UK Limited).

Fetal HPC Transplantation. After 2 days of culture, the cell clusters were resuspended in 400 μL of PBS and transplanted into the livers. After anesthetization of the recipient mice with intraperitoneal injection of sodium pentobarbital (10 mg/g), a 70% partial hepatectomy was

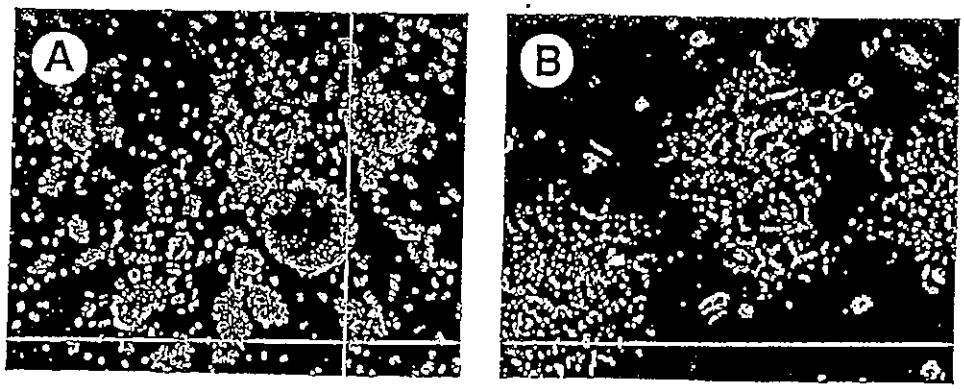

Fig. 1. Cell aggregates formed during suspension culture and isolated cell colonies were cultured on type I collagen-coated culture plates. Phase contrast images of (A) cell aggregates formed during 12-hour suspension culture after fetal liver digestion and (B) extending isolated cell colonies 24 hours after inoculation on type I collagen-coated culture plates. Original magnification, ×200.

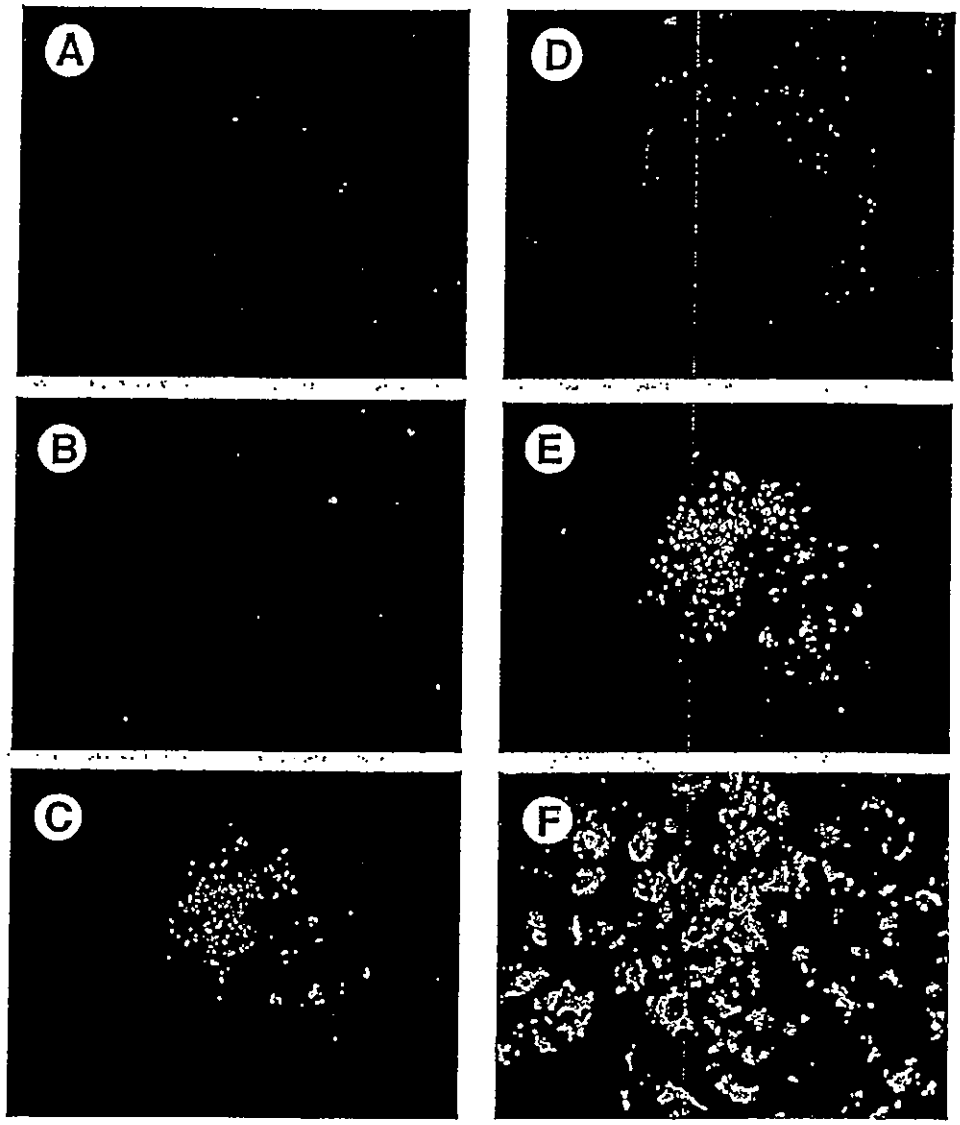

Fig. 2. Immunocytochemistry for isolated cell colonies. Fluorescent microscopy images of isolated cell colonies stained for (A and B) AFP, (C) ALB, (D) CK19. **Red and green fluorescence** represents immunocytologically positive cells. **Blue fluorescence** indicates cell nuclei stained by 4′, 6-diamidino-2-phenylindole. (E) The merged images of (C) and (D) represent ALB and CK19 expression patterns in the isolated cell colony. (F) The high-power field image of (E) represents ALB and CK19 double-positive cells (**yellow cells**). Original magnification, ×200 (A, C, D, and E) and ×400 (B and F). These results were reproducible in every immunocytochemistry analysis performed on more than 50 colonies.

performed. Then, a 200-μL suspension of HPC aggregates was slowly injected with a 27-gauge needle into one site of the exposed remnant liver of each mouse. The injected site of the recipient liver was pressed with a cotton stick for 5 minutes immediately after transplantation to prevent bleeding or cell leakage.

Fluorescent Microscopic Examination of Liver Tissue. Ten days after the fetal HPC transplantation, the recipient liver tissues were harvested and incubated in paraformaldehyde at 4°C for 7 hours. After rinsing with PBS, they were dehydrated in acetone at 4°C for 1 hour and rinsed in PBS. Thereafter, the liver tissues were put into Tissue-Tek O.C.T. Compound (Sakura Finetechnical Co., Ltd., Tokyo, Japan) and frozen at −80°C for more than 24 hours, and then sectioned with a Cryostat (Aloka Co., Ltd., Tokyo, Japan). The sections were covered with 50% glycerol on silane-coated glass plates, and the expression of DsRed representing the exogenous gene transfected into the fetal HPC was investigated under the fluorescent microscope. Albumin expression in the transplanted fetal HPCs was also confirmed by albumin staining with the FITC-labeled antibody. Four recipient mice in total were analyzed.

Statistical Analysis. Statistical analysis was performed for ^{3}H-thymidine incorporation and transfection efficiency determination by the Student's t test. A value of $P < .05$ was considered significant.

Results

Isolation and Characterization of Fetal HPC. In every suspension culture performed (n = 20), the largest cells derived from fetal liver tissues adhered to each other to consequently form floating cell aggregates, and al-

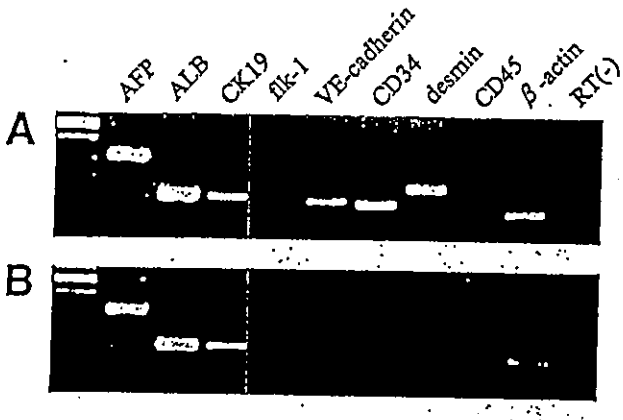

Fig. 3. RT-PCR analysis for lineage marker expression on isolated cells. (A) Lineage marker analysis for dissociated fetal liver before selection of cell aggregates by RT-PCR. (B) Lineage marker analysis for cell aggregates by RT-PCR. This experiment was reproduced 4 times.

though fibroblasts adhered to the Petri dish, hematopoietic cells remained as floating single cells (Fig. 1A). The difference in size caused by the formation of cell aggregates enabled their selection from other single-cell populations depending on gravity sedimentation. When the cell aggregates were inoculated onto type I collagen-coated culture plates and cultured for 24 hours, they formed monolayer cell colonies (Fig. 1B). The cells in the colonies appeared morphologically uniform and cuboidal in shape, and possessed large nuclei and highly granulated cytoplasm. These characteristics are compatible with fetal HPCs. To characterize these cells biologically, marker gene expression was evaluated. In immunocytochemistry, almost all of the cells in the colonies were stained for AFP (Fig. 2A and B), but only partially for ALB (Fig. 2C) and CK19 (Fig. 2D). Interestingly, albumin was expressed

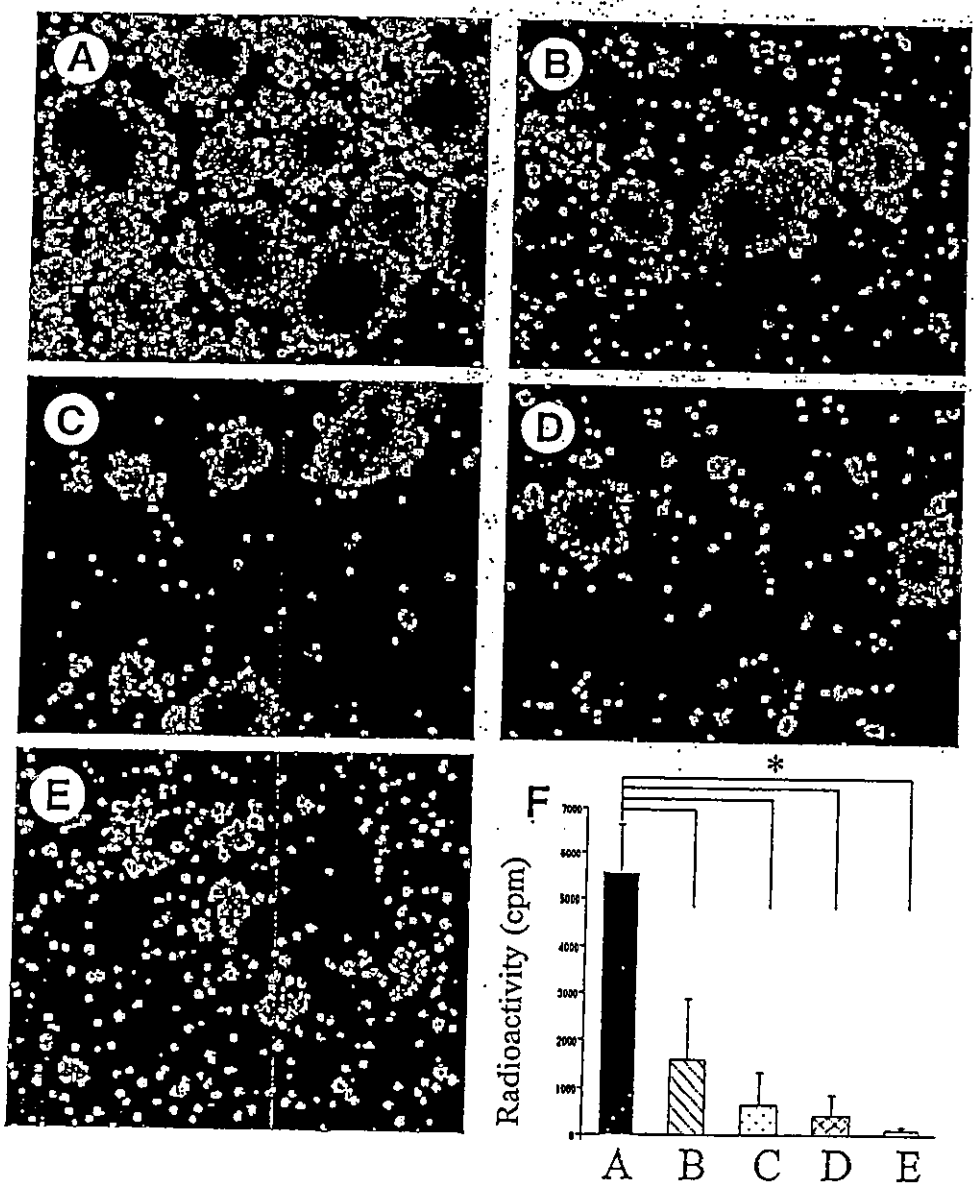

Fig. 4. Fetal HPC aggregate formation and ^{3}H-thymidine incorporation compared among different culture media. Phase contrast images of fetal HPC aggregate formation in different culture media. (A) RPMI 1640 with FCS, dHGF, and insulin. (B) RPMI 1640 with FCS and dHGF. (C) RPMI 1640 with FCS and insulin. (D) RPMI 1640 with FCS. (E) RPMI 1640. Original magnification, ×200. (F) The radioactivity of ^{3}H-thymidine incorporated into HPCs in the culture media described above. HPCs were inoculated in the same cell number in all experiments. The vertical axis represents radioactivity (cpm) ($n = 3$, $^{*}P < .05$).

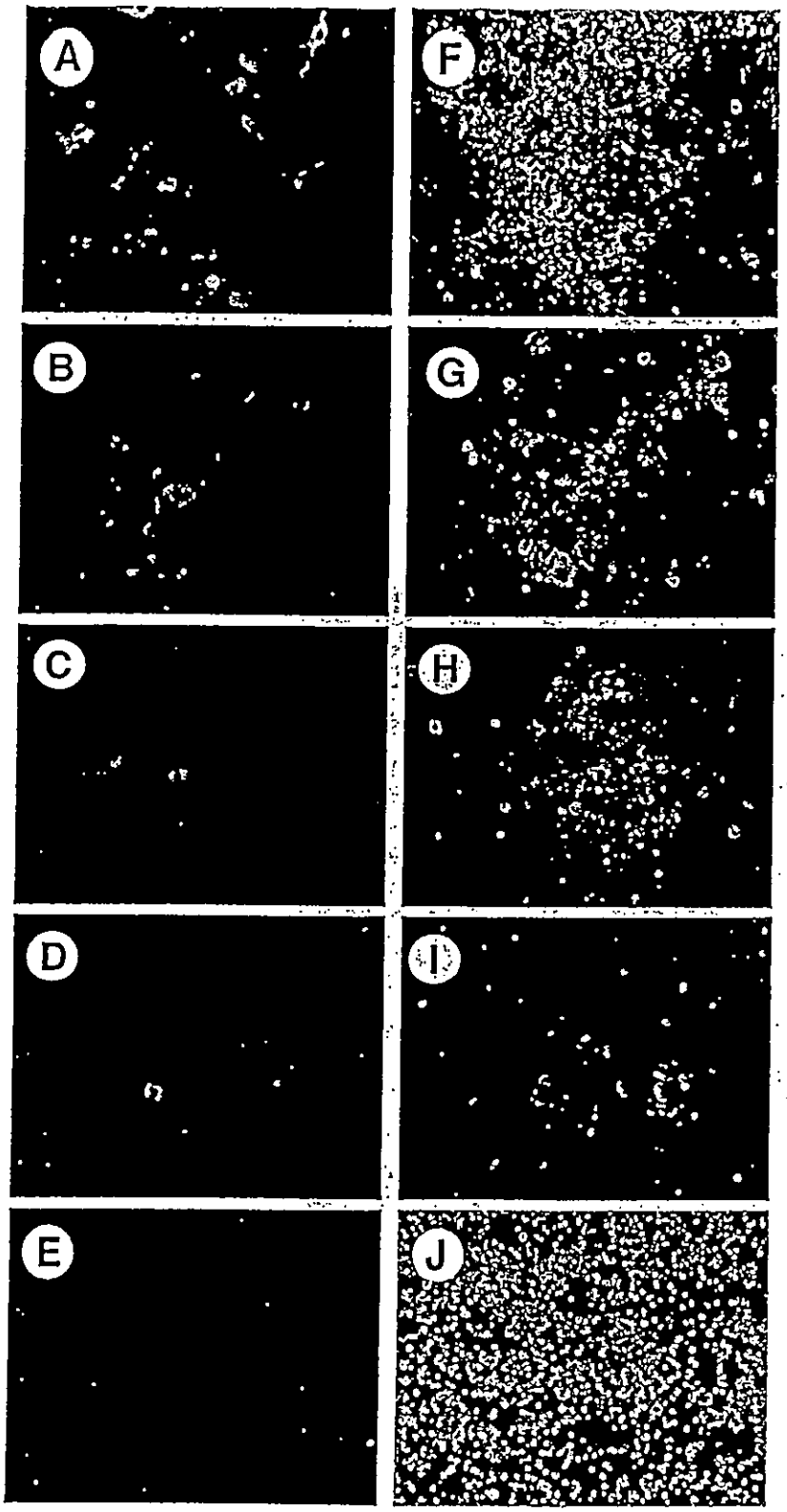

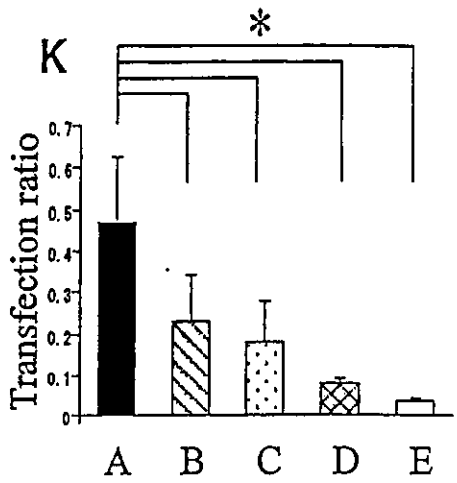

Fig. 5. DsRed expression in fetal HPCs compared among different culture media. (A-E) Fluorescent microscopy images of DsRed expression in fetal HPCs compared among different culture media as described in Fig. 4. (F-J) The corresponding phase contrast images for A-E, respectively. These results were reproducible (n = 10). Original magnification, ×200. (K) The ratios of DsRed-expressing cells were compared among different culture media as described in Fig. 4 (n = 3, *$P < .05$).

more strongly in the cells located at the central portion of each colony, whereas CK19 was expressed more strongly at the periphery (Fig. 2C, D, and E), and double-positive cells were detected (Fig. 2E and F). Additionally, RT-PCR showed that the cells in the colonies expressed mRNA of AFP, ALB, and CK19, whereas the expressions of mesenchymal marker fetal liver kinase-1, vascular cell marker VE-cadherin and CD34, stellate cell marker

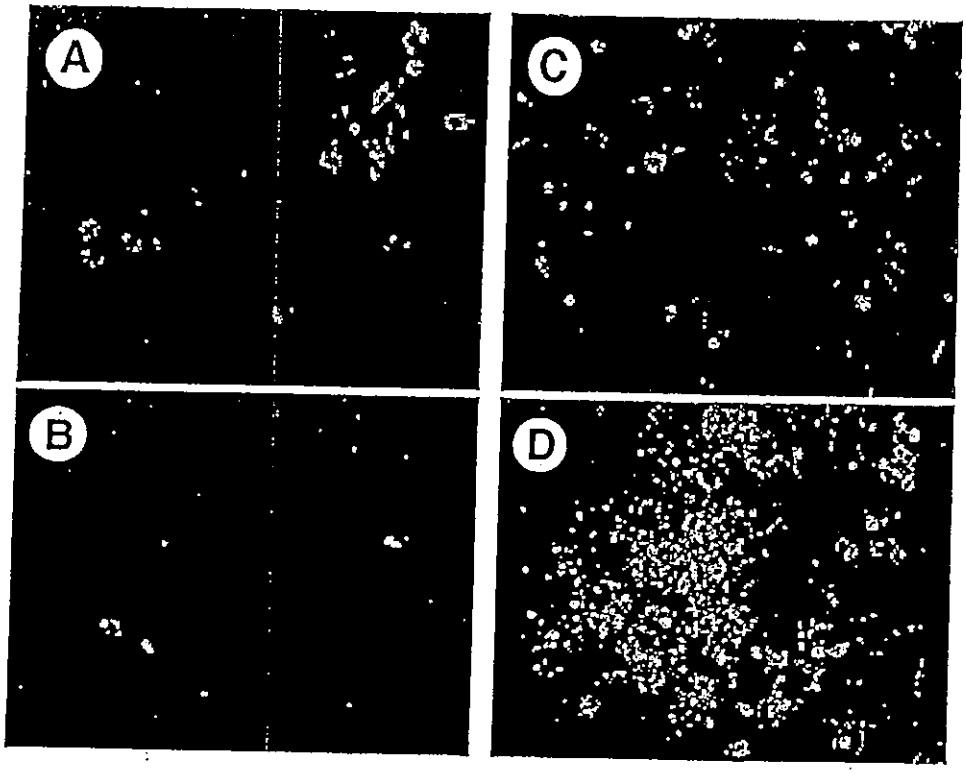

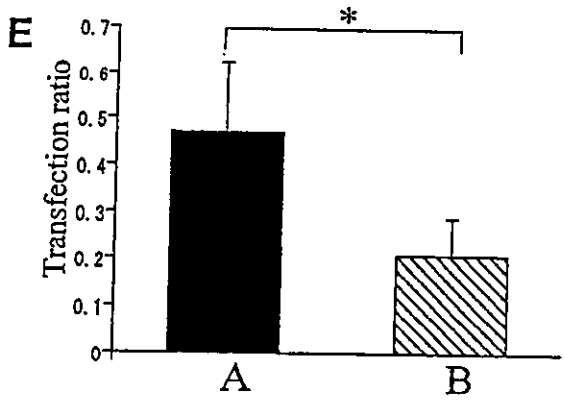

Fig. 6. DsRed expression in fetal HPCs in relation to timing of gene transfection. Fluorescent microscopy images of DsRed expression in fetal HPCs transfected (A) concomitantly with the beginning of suspension culture and (B) 6 hours after the beginning of suspension culture. (C) and (D) are the corresponding phase contrast images for (A) and (B), respectively. Original magnification, ×200. (E) The ratios of DsRed-expressing cells in the case of (A) and (B) ($n = 3$, $^*P < .05$).

desmin, and hematopoietic marker CD45 were not detected (Fig. 3). Consequently, the cells in the colonies proved to be fetal HPCs.

^{3}H-Thymidine Incorporation. It is generally believed that cells in the replicating phase incorporate exogenous genes more feasibly than those in the quiescent phase. To establish the optimal growth culture conditions for highly efficient gene transfection and expression, we first compared the growth of fetal HPCs among several compositions of culture media (Fig. 4A-E). It was most efficient in RPMI 1640 with 10% FCS, 10 ng/mL dHGF, and 600 ng/mL insulin. When ^{3}H-thymidine incorporation into fetal HPCs was investigated, it was 50-fold higher in this media compared with RPMI 1640 alone (Fig. 4F).

Exogenous Gene Transfection. When the efficacy of DsRed gene transfection was compared among the culture media tested for ^{3}H-thymidine incorporation, it was also the highest in RPMI 1640 with 10% FCS, 10 ng/mL dHGF, and 600 ng/mL insulin as expected from the ^{3}H-thymidine incorporation experiments (Fig. 5A-E). Furthermore, the efficacy of DsRed gene transfection was compared in relation to the timing of gene transfection under the determined culture media and transfection reagents. A higher efficacy was detected in the case of gene transfection concomitantly performed at the beginning of suspension culture (Fig. 6A) than that performed 6 hours after formation of the cell aggregates (Fig. 6B).

Considering all these results, we finally determined the best conditions for gene transfection to fetal HPCs, that

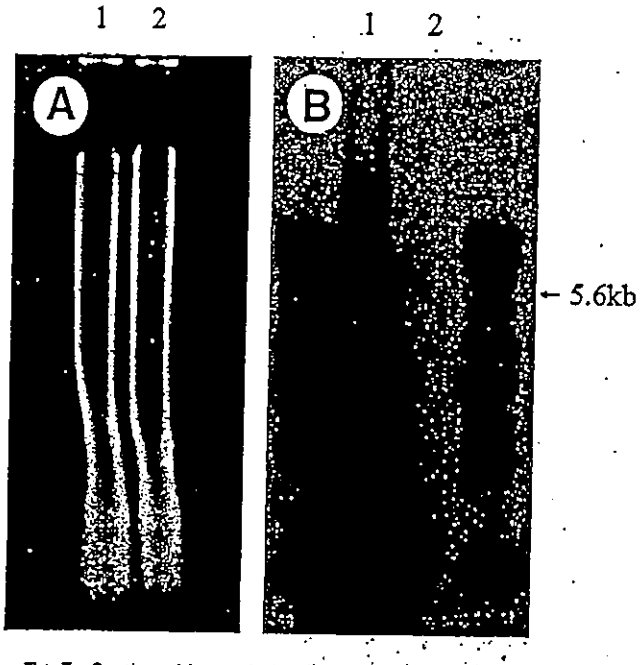

Fig. 7. Southern blot analysis of exogenous gene integration. DsRed probe labeled with alkaline phosphatase was hybridized to the digested genomic DNA extracted from DsRed-gene transferred HPCs (**lane 1**) and nontransferred HPCs (**lane 2**). (A) Electrophoresis of the digested genomic DNA representing the same amount of DNA was applied between **lane 1** and **lane 2**. (B) The chemiluminescence of the hybridized DsRed probe.

is, transfecting the DsRed gene at the beginning of suspension culture and culturing in RPMI 1640 with 10% FCS, 10 ng/mL dHGF, and 600 ng/mL insulin. In this situation, the exogenous DsRed gene was expressed in 85.4% ± 4.2% of cell aggregates and in 45.2% ± 12.3% of fetal HPCs. This outstanding efficiency led us to investigate the integration of the DsRed gene under the determined condition as described above. In the Southern blot analysis, the chemiluminescence was reproducibly detected only in the sample of DsRed-transferred HPCs in a smear fashion representing diverse integration. The vector size band (5.6 kb) was also detected (Fig. 7). This vector size band represented tandem integration into the genome of HPCs because it was not detected when the same genome DNA was not digested with *Hind*III (data not shown).

Fetal HPC Transplantation After In Vitro *Gene Transfer.* On the basis of the above results, we examined the possibility of using exogenous gene-transferred fetal HPCs as a vector for cellular gene therapy. Ten days after transplantation of the gene-transferred fetal HPCs into the liver, they settled in the recipient regenerating liver tissue concomitantly maintaining continuous DsRed-gene expression (Fig. 8A and B) reproducibly in all of the cases investigated. The transplanted fetal HPCs also maintained one of their own hepatic functionalities, which was confirmed by their albumin expression (Fig. 8C and D).

Discussion

Until recently, fetal HPCs were isolated using collagenase digestion and low-speed centrifugation according to the method of Seglen et al.[22] However, because the size of HPCs in the fetus resembles that of nonparenchymal cells, their contamination could not be excluded if solely dependent on centrifugation, which should discriminate cell populations according to their size. Contaminating fibroblasts easily overwhelm HPCs during culture. This makes it difficult to obtain pure fetal HPCs to evaluate their transfection efficacy in gene transfection experiments. However, to assess the possibility of HPC use as a vector for cellular gene therapy, a purification method and culture system capable of evaluating transient gene expression in pure fetal HPCs would be indispensable. Furthermore, if the selection of HPCs integrating exogenous genes in their genome is intended, further long-term culture would be necessary. Regarding the purification of HPCs, Suzuki et al. and Kubota et al. have recently reported a method using a fluorescent-activated cell sorter and succeeded in producing a clonal culture.[12,23] However, to achieve highly efficient gene transfection into fetal HPCs, we considered it necessary to simplify the isolation and transfection system because gene transfection and expression generally depend on the cell viability and cell cycle. Fluorescent-activated cell-sorted fetal HPCs were lower in cell viability than those immediately after liver digestion in our preliminary experiments. Therefore, we intended to develop a new isolating method free from mechanical stress for fetal HPCs. The purification of fetal HPCs was confirmed by the immunocytochemistry and RT-PCR results. This was possible because the fetal HPCs were incorporated into the cell aggregates, which were larger than single cells, and this difference led to discrimination of the fetal HPCs from the other cell populations by simple gravity sedimentation. In our other experiments, these cell aggregates proved to depend on homophilic binding of cell-adhesion molecules, such as E-cadherin.[23a] Considering that the cell aggregates are formed depending on the homophilic cell-to-cell adhesion, only the cells in the fetal liver rich enough in population to encounter their companions expressing counterparts of homophilic binding molecule during suspension culture may be able to participate in cell aggregation. According to the biological features of E-cadherin as an endodermal marker in the liver,[24] it is of no surprise that our system resulted in fetal HPC selection of high purity. This enabled a precise investigation of the efficacy of gene transfection and long-term culture of fetal HPCs

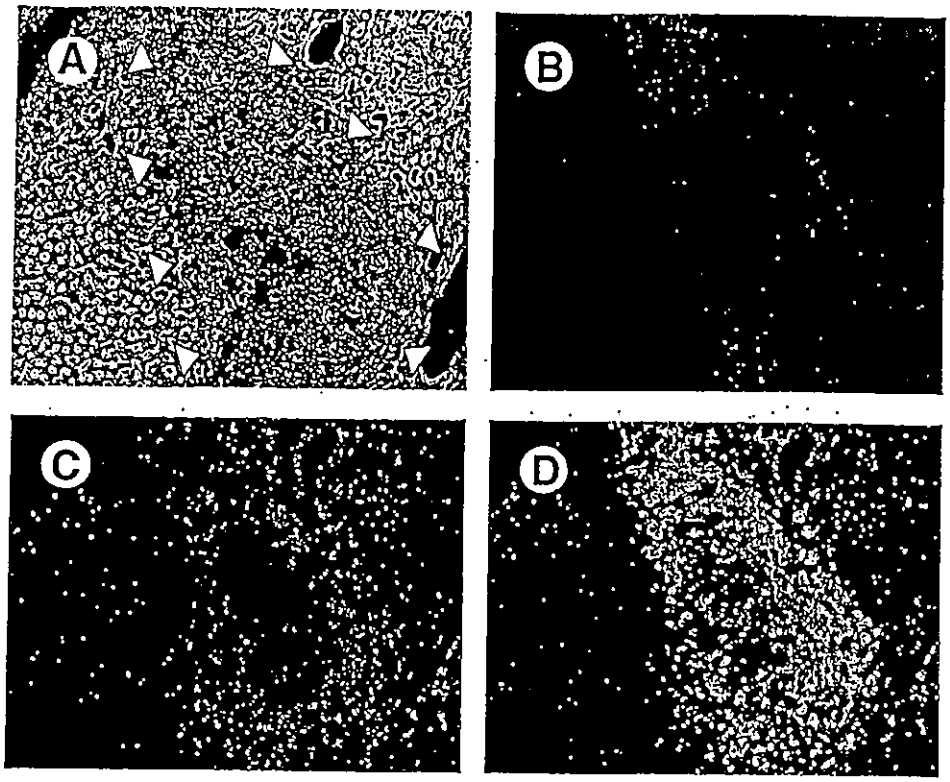

Fig. 8. DsRed expression and endogenous albumin synthesis in cells transplanted to the liver tissue. (A) Recipient liver tissue transplanted with gene-transfected HPCs (**arrowheads**). (B and C) The corresponding fluorescent microscopic images. **Red fluorescence** represents transfected DsRed gene expression, and **green fluorescence** represents albumin expression. (D) The merged images of (B) and (C). Original magnification, ×100. These results were reproducible in all of the investigated cases ($n = 4$).

in high purity, which is a prerequisite for the selection of stable transfectants by drug resistance.

The main point we would like to emphasize in this article is that this method enabled highly efficient *in vitro* gene transfer independent of viral vectors, and we obtained a mass of gene-transferred HPCs with high viability. This is desirable for the use of HPCs as a gene-delivery vector. According to our system, a higher efficacy of gene transfection was achieved than that achieved in fetal HPCs selected by fluorescent activated cell sorter (data not shown). We believe this resulted from the higher viability maintained because of nonmechanical selection. The exogenous gene expression was comparatively high even when compared with that of other reports on transfection experiments using hepatic lineage cells.[25-26] This may be attributable to the following reasons. Fetal HPCs divide more frequently than adult hepatocytes. For this reason, exogenous genes may be easily transferred into them. Additionally, from the fact that the highest efficacy of gene transfer was achieved when the DsRed gene was transfected concomitantly with the beginning of suspension culture, the lack of any surrounding extracellular matrix may allow exogenous genes to access fetal HPCs more easily. Furthermore, this higher expression compared with previous methods may be partially attributable to incorporation of exogenous genes into the genome of HPCs. In fact, the results of the Southern blot analysis presented direct evidence of a considerable number of the exogenous gene copies integrated into fetal HPCs in our transfection system. When fetal HPCs integrating exogenous genes in their genome were selected based on drug resistance, they could be purified to over 97% (data not shown). This suggests that only the exogenous-gene-expressing HPCs may be purified, expanded, and then prepared for transplantation by our system. Our results also showed that the gene expression was maintained *in vivo* in the transplanted liver and the transplanted fetal HPCs settled in the liver tissue, retaining the function of albumin synthesis. Although this is theoretically a matter of fact, our work is the first to present evidence showing the possibility of using HPCs as a nonviral vector. Considering the recent evidence suggesting the potential risk of using adenoviral vectors, our results may lead to the development of an alternative system for gene delivery realizing "cellular gene therapy" against liver diseases in the foreseeable future. From this point of view, we are now applying this system to human fetal HPCs.

Acknowledgment: The authors thank Snow Brand Milk Products Co., Ltd., for providing the deleted form of hepatocyte growth factor.

References

1. Bilir BM, Guinette D, Karrer F, Kumpe DA, Krysl J, Stephens J, McGavran L, et al. Hepatocyte transplantation in acute liver failure. Liver Transpl 2000;6:32-40.

2. Chowdhury JR, Chowdhury NR, Strom SC, Kaufman SS, Horslen S, Fox IJ. Human hepatocyte transplantation: gene therapy and more? Pediatrics 1998;102:647-648.
3. Fox IJ, Chowdhury JR, Kaufman SS, Goertzen TC, Chowdhury NR, Warkentin PI, Strom SC, et al. Treatment of the Crigler-Najjar syndrome type I with hepatocyte transplantation. N Engl J Med 1998;338:1422-1426.
4. Strom SC, Chowdhury JR, Fox IJ. Hepatocyte transplantation for the treatment of human disease. Semin Liver Dis 1999;19:39-48.
5. Kobayashi N, Ito M, Nakamura J, Cai J, Hammel JM, Fox IJ. Hepatocyte transplantation improves liver function and prolongs survival in rats with decompensated liver cirrhosis. Transplant Proc 1999;31:428-429.
6. Kobayashi N, Fujiwara T, Westerman KA, Inoue Y, Sakaguchi M, Noguchi H, Leboulch P, et al. Prevention of acute liver failure in rats with reversibly immortalized human hepatocytes. Science 2000;287:1258-1262.
7. Lee B, Dennis JA, Healy PJ, Mull B, Pastore L, Yu H, Beaudet AL, et al. Hepatocyte gene therapy in a large animal: a neonatal bovine model of citrullinemia. Proc Natl Acad Sci U S A 1999;96:3981-3986.
8. Veyron P, Touraine JL. Fetal liver cell transplantation: survival of grafted BALB/c lysosomal storage disease mice. Transplant Proc 1990;22:2253-2254.
9. Vogels BA, Maas MA, Bosma A, Chamuleau RA. Significant improvement of survival by intrasplenic hepatocyte transplantation in totally hepatectomized rats. Cell Transplant 1996;5:369-378.
10. Vroemen JP, Buurman WA, Heirwegh KP, van der Linden CJ, Kootstra G. Hepatocyte transplantation for enzyme deficiency disease in congenic rats. Transplantation 1986;42:130-135.
11. Weglarz TC, Degen JL, Sandgren EP. Hepatocyte transplantation into diseased mouse liver. Kinetics of parenchymal repopulation and identification of the proliferative capacity of tetraploid and octaploid hepatocytes. Am J Pathol 2000;157:1963-1974.
12. Kubota H, Reid LM. Clonogenic hepatoblasts, common precursors for hepatocytic and biliary lineages, are lacking classical major histocompatibility complex class I antigen. Proc Natl Acad Sci U S A 2000;97:12132-12137.
13. Bumgardner GL, Li J, Heininger M, Ferguson RM, Orosz CG. In vivo immunogenicity of purified allogeneic hepatocytes in a murine hepatocyte transplant model. Transplantation 1998;65:47-52.
14. Geissler EK, Graeb C, Tange S, Guba M, Jauch KW, Scherer MN. Effective use of donor MHC class I gene therapy in organ transplantation: prevention of antibody-mediated hyperacute heart allograft rejection in highly sensitized rat recipients. Hum Gene Ther 2000;11:459-469.
15. Kamada N, Davies HS, Roser B. Reversal of transplantation immunity by liver grafting. Nature 1981;292:840-842.
16. Bumgardner GL, Li J, Prologo JD, Heininger M, Orosz CG. Patterns of immune responses evoked by allogeneic hepatocytes: evidence for independent co-dominant roles for CD4+ and CD8+ T-cell responses in acute rejection. Transplantation 1999;68:555-562.
17. Scherer MN, Graeb C, Tange S, Dyson C, Jauch KW, Geissler EK. Immunologic considerations for therapeutic strategies using allogeneic hepatocytes: hepatocyte-expressed membrane-bound major histocompatibility complex class I antigen sensitizes while soluble antigen suppresses the immune response in rats. HEPATOLOGY 2000;32:999-1007.
18. Ito Y, Matsui T, Kamiya A, Kinoshita T, Miyajima A. Retroviral gene transfer of signaling molecules into murine fetal hepatocytes defines distinct roles for the STAT3 and ras pathways during hepatic development. HEPATOLOGY 2000;32:1370-1376.
19. Nakamura T, Nawa K, Ichihara A. Partial purification and characterization of hepatocyte growth factor from serum of hepatectomized rats. Biochem Biophys Res Commun 1984;122:1450-1459.
20. Nakamura T, Nishizawa T, Hagiya M, Seki T, Shimonishi M, Sugimura A, Shimizu S, et al. Molecular cloning and expression of human hepatocyte growth factor. Nature 1989;342:440-443.
21. Hirose T, Terajima H, Yamauchi A, Kinoshita K, Furuke K, Gomi T, Yamaoka Y, et al. Oxygen dependency of epidermal growth factor receptor binding and DNA synthesis of rat hepatocytes. J Hepatol 1997;27:1081-1088.
22. Seglen PO. Preparation of isolated rat liver cells. Methods Cell Biol 1976; 13:29-83.
23. Suzuki A, Zheng Y, Kondo R, Kusakabe M, Takada Y, Fukao K, Taniguchi H, et al. Flow-cytometric separation and enrichment of hepatic progenitor cells in the developing mouse liver. HEPATOLOGY 2000;32:1230-1239.
23a. Hirose T, Yasuchika K, Fujikawa T, Fujii H, Oe S, Azuma H, Ikai I, et al. "Blastosphere": a new culture method for human fetal hepatic progenitor cells. Gastroenterology 2002;120(Suppl 1):A-542.
24. Takeichi M. The cadherins: cell-cell adhesion molecules controlling animal morphogenesis. Development 1988;102:639-655.
25. Wilke M, Bijma A, Timmers-Reker AJ, Scholte BJ, Sinaasappel M. Complementation of the genetic defect in Gunn rat hepatocytes in vitro by highly efficient gene transfer with cationic liposomes. Gene Ther 1997;4: 1305-1312.
26. Rangarajan PN, Vatsala PG, Ashok MS, Srinivas VK, Habibullah CM, Padmanaban G. Non-viral ex vivo hepatic gene transfer by in situ lipofection of liver and intraperitoneal transplantation of hepatocytes. Gene 1997;190:217-221.

Journal of Cellular Biochemistry 87:16–28 (2002)

Morphological Changes Induced by Extracellular Matrix Are Correlated with Maturation of Rat Small Hepatocytes

Shinichi Sugimoto,[1,3] Toshihiro Mitaka,[1]* Shinichiro Ikeda,[1,2] Keisuke Harada,[1,2] Iwao Ikai,[3] Yoshio Yamaoka,[3] and Yohichi Mochizuki[1]

[1]Department of Pathology, Cancer Research Institute, Sapporo Medical University School of Medicine, Sapporo, Japan
[2]Department of Surgery, Sapporo Medical University School of Medicine, Sapporo, Japan
[3]Department of Gastroenterological Surgery, Kyoto University Medical School, Kyoto, Japan

Abstract Small hepatocytes (SHs), which are known to be hepatic progenitor cells, were isolated from an adult rat liver. SHs in a colony sometimes change their shape from small to large and from flat to rising/piled-up. The aim of the present study is to clarify whether the alteration of cell shape is correlated with the maturation of SHs and whether extracellular matrix (ECM) can induce the morphological changes of SHs. We used liver-enriched transcription factors (LETFs) such as hepatocyte nuclear factor (HNF) 4α, HNF6, CCAAT/enhancer binding proteins (C/EBP) α, and C/EBPβ, tryptophan 2,3-dioxygenase (TO), and serine dehydratase (SDH) as markers of hepatic maturation. To enrich the number of SH colonies, the colonies were isolated from dishes and replated. Replated colonies proliferated and the average number of cells per colony was about five times larger at day 9 than at day 1. When the cells were treated with laminin, type IV collagen, a mixture of laminin and type IV collagen, Matrigel™ or collagen gel (CG), only the cells treated with Matrigel dramatically changed their shape within several days and had reduced growth activity, whereas the cells treated with other ECM did not. HNF4α, HNF6, C/EBPα, C/EBPβ, and TO were well expressed in the cells treated with Matrigel. Furthermore, addition of both glucagon and dexamethasone dramatically induced the expression of SDH mRNA and protein in the cells treated with Matrigel. In conclusion, morphological changes of SHs may be correlated with hepatic maturation and basement membrane (BM)-like structure may induce the morphological changes of SHs. J. Cell. Biochem. 87: 16–28, 2002. © 2002 Wiley-Liss, Inc.

Key words: liver-enriched transcription factors; Matrigel; serum proteins; growth; hepatic nonparenchymal cells

Small hepatocytes (SHs) have been identified as proliferating cells with hepatic characteristics [Mitaka et al., 1992, 1993; Tateno and Yoshizato, 1996]. Recently, we showed that a single SH could clonally proliferate and form a large colony [Mitaka et al., 1995, 1999]. Some SH colonies changed their shapes from flat to rising/piled-up cells with time in culture. The rising/piled-up cells were large and tall, possessed many mitochondria, peroxisomes with a crystalline nucleoid, and glycogen granules [Mitaka et al., 1999]. In such colonies nonparenchymal cells (NPCs) invaded under the colony and an accumulation of extracellular matrix

Abbreviations used: AP, alkaline phosphatase; Asc2P, ascorbic acid 2-phosphate; BC, bile canaliculi; BM, basement membrane; C/EBPα, CCAAT/enhancer binding protein α; Cx, connexin; DAB, 3′-diaminobenzidine; DAPI, 6-diamino-2-phenylindole; DMEM, Dulbecco's modified Eagle's medium; DMSO, dimethylsulfoxide; ECM, extracellular matrix; EGF, epidermal growth factor; EHS, Engelbreth–Holm–Swarm; ELISA, enzyme-linked immunosorbent assay; FBS, fetal bovine serum; HNF, hepatocyte nuclear factor; LECs, liver epithelial cells; LETFs, liver-enriched transcription factors; MHs, mature hepatocytes; NPCs, nonparenchymal cells; PAGE, polyacrylamide gel electrophoresis; PCNA, proliferating cell nuclear antigen; SDH, serine dehydratase; SHs, small hepatocytes; TEM, transmission electron microscopy; TO, tryptophan 2,3-dioxygenase.

© 2002 Wiley-Liss, Inc.

Grant sponsor: Ministry of Education, Science, Sports and Culture Japan; Grant numbers: 10670213 (to TM), 12670211 (to TM), 11470244 (to II), 1247243 (to YM); Grant sponsor: Health Sciences Research Grant; Grant sponsor: Research on Human Genome, Tissue Engineering Food Biotechnology.

*Correspondence to: Toshihiro Mitaka, Department of Pathology, Cancer Research Institute, Sapporo Medical University School of Medicine, Chuo-Ku, S-1, W-17, Sapporo 060-8556, Japan. E-mail: tmitaka@sapmed.ac.jp

Received 28 May 2002; Accepted 17 June 2002

DOI 10.1002/jcb.10274

Published online 17 July 2002 in Wiley InterScience (www.interscience.wiley.com).

(ECM) between hepatocytyes and NPCs was observed. Therefore, we suspected that SHs could differentiate into mature hepatocytes (MHs) that interacted with hepatic NPCs and ECM [Mitaka et al., 1999].

For the purpose of maintaining the differentiated functions, many researchers have used various substances and changed culture conditions through the use of nicotinamide [Inoue et al., 1989; Mitaka et al., 1991], phenobarbital [Miyazaki et al., 1985], dimethylsulfoxide [DMSO; Isom et al., 1985], ECM [Rojkind et al., 1980; Bissell et al., 1987; Ben-Ze'ev et al., 1988; Schetz et al., 1988; Dunn et al., 1992], coculture with NPCs [Guguen-Guillouzo, 1986], and spheroid formation [Koide et al., 1989; Ingber, 1993; Iredale and Arthur, 1994; Rojkind and Greenwel, 1994]. In such experiments, the maintenance of liver-specific functions of the cells was evaluated by expression of mRNAs and/or proteins such as serum proteins, gap junctional proteins like connexin 32 (Cx32) and Cx26, tryptophan 2,3-dioxygenase (TO), and serine dehydratase (SDH). Many genes of those liver-specific proteins are known to be mainly regulated by liver-enriched transcription factors (LETFs) such as CCAAT/enhancer binding protein (C/EBP) α and C/EBPβ, and hepatocyte nuclear factor (HNF) 1α, HNF3α, HNF4α, and HNF6 [Tian and Schibler, 1991; Kuo et al., 1992; Cereghini, 1996; Uzma and Costa, 1996]. Primary hepatocytes cultured on Matrigel™, which is Engelbreth–Holm–Swarm (EHS) sarcoma-derived matrix, maintained some differentiated functions such as albumin, transthyretin, and apolipoprotein A-I production and kept the transcription of HNF1α and HNF4 mRNAs [Nagaki et al., 1995; Oda et al., 1995]. It has been emphasized that cell shape is a key factor to regulate the growth, differentiation, and survival of hepatocytes [Walt, 1986; Maher, 1988]. ECM was reported to be able to modulate the shapes of cultured hepatocytes [Bissell et al., 1987; Maher, 1988; Koide et al., 1989]. Ben-Ze'ev et al. [1988] suggested that cell shape might be a primary regulator of tissue-specific gene expression and that cytoskeletal components might interact directly with the nuclear matrix to affect gene transcriptional rates.

In the present study, we showed that the addition of Matrigel could dramatically change the shapes of the cells as well as the structure of the colonies. In addition, the changes of cell shape were correlated with the expression of hepatic differentiated proteins. To clarify why Matrigel could induce the morphological changes of SHs, we examined the effects of various ECM and growth factors, which are included in Matrigel, on SHs in the colonies. Not only laminin, type IV collagen, a mixture of laminin and type IV collagen, and collagen gel (CG) but also basic fibroblast growth factor (bFGF), pletelet-derived growth factor (PDGF), nerve growth factor (NGF), and transforming growth factor β (TGFβ) did not affect the alteration of cellular morphology. Thus, we hypothesize that morphological changes of SHs may be correlated with hepatic maturation and that the formation of the basement membrane (BM)-like structure may be responsible in part for the beneficial effect of those morphological changes of the cells.

MATERIALS AND METHODS

Isolation and Culture of Hepatic Cells

Male Sprague–Dawley rats (Shizuoka Laboratory Animal Center, Hamamatsu, Japan), weighing 250–400 g, were used to isolate SHs. All animals received humane care and the experimental protocol was approved by the Committee of Laboratory Animals according to University guidelines. Details of the isolation and culture procedure of the cells were previously described [Mitaka et al., 1999]. Finally, 2×10^5 viable cells/ml were plated on dishes (1.5 ml/35-mm dish; 4 ml/60-mm dish; 10 ml/100-mm dish; Corning Glass Works, Corning, NY) and cultured in Dulbecco's modified Eagle's medium (DMEM; GIBCO Laboratories, Grand Island, NY) supplemented with 20 mM HEPES, 25 mM $NaHCO_3$, 30 mg/L L-proline, 10% fetal bovine serum (HyClone, Logan, UT), 10 mM nicotinamide (Katayama Chemical Co., Osaka, Japan), 1 mM ascorbic acid 2-phosphate (Asc2P; Wako Pure Chem, Tokyo, Japan), 10 ng/ml epidermal growth factor (EGF; Collaborative Research, Inc., Lexington, MA), hormone, and antibiotics. After 4 days of culture, 1% DMSO (Aldrich Chem Co., Milwaukee, WI) was added to the medium. Medium was replaced every other day.

Replating of Small Hepatocyte Colonies

When SHs proliferated and formed colonies consisting of 15–40 cells (8–12 days after plating), the colonies were detached from dishes and replated on new dishes. Cells were rinsed

with PBS and then treated with 0.02% EDTA/PBS for 1 min. The cells were then treated with cell dissociation solution (Sigma Chem Co., St. Louis, MO) for 5 min at 37°C. After addition of DMEM supplemented with 10% FBS in the dish, SH colonies were collected into conical tubes and the cell suspension was centrifuged at 50*g* for 5 min. The pellet was resuspended in the medium. The number of viable colonies was counted and the colonies were plated on rat tail collagen-coated dishes [Michalopoulos and Pitot, 1975]. Four to five hours after plating, the medium was replaced with the serum-free medium.

Addition of ECM or Growth Factors

At 11 days after replating, the cells were treated with various ECM such as laminin, type IV collagen, a mixture of laminin and type IV collagen, fibronectin, CG, or growth factor-reduced Matrigel (Becton Dickinson Labware, Bedford, MA). The concentrations of individual ECM components used were similar to those in Matrigel (the manufacturer's data). Forty-eight hours after the treatment, the medium was replaced with fresh medium without ECM. On the other hand, growth factors such as TGF-β, PDGF (Genzyme/Techne, Minneapolis, MN), βNGF (PeproTech EC Ltd., London, United Kingdom), and bFGF (Dainippon Pharm Ltd., Osaka, Japan) were added to the medium at day 11. The concentrations of the growth factors were maximally 10 times larger than in Matrigel. Fresh growth factors were added to the medium at the time of medium change.

Photographs of Cells

The same fields of dishes identified by needle marks were digitally recorded by using a phase-contrast microscope (Olympus Optical Co., Tokyo, Japan) equipped with a CCD camera (Roper Scientific, Trenton, NJ).

Immunostaining of Cultured Cells

Cells were fixed with cold absolute ethanol. Mouse anti-proliferating cell nuclear antigen (PCNA; DAKO, Copenhagen, Denmark) and anti-cytokeratin (CK) 8 antibodies (Amersham Corp., Buckinghamshire, United Kingdom) were used as the primary antibodies, followed by the avitin–biotin peroxidase complex method (Vectastain ABC Elite Kit; Vector Laboratories, Inc., Burlingame, CA). 3′-Diaminobenzidine (DAB; Tokyo Kasei Industries, Tokyo, Japan) was used as a substrate. The cells were then counter-stained with hematoxylin. For counting the number of the cells in a colony, immunocytochemistry procedures for CK8 and PCNA were used to identify SHs and to examine the growth activity of the cells, respectively.

For triple immunofluorescent staining, we used a rabbit anti-C/EBPα, a goat anti-HNF4α, or a goat anti-HNF6 antibody (Santa Cruz Biotechnology, Inc., Santa Cruz, CA) and a mouse anti-E-cadherin antibody (Transduction Laboratory, Lexington, KY) as the primary antibody. Alexa^{488}-conjugated anti-rabbit and goat IgG antibodies or Alexa^{594}-conjugated anti-mouse IgG (Mol Probe, Eugene, OR) as the secondary antibody were also used. 6-Diamino-2-phenylindole (DAPI) was used as a marker of nuclei. The samples were analyzed using the CELL-Scan system (Scanalytics, Billerica, MA). The details of the procedure were previously described [Mitaka et al., 1999].

Enzyme-Linked Immunosorbent Assay (ELISA) for Rat Albumin

The medium was collected every 48 h at the time of medium replacement and centrifuged at $1 \times 10^4 g$ for 10 min. The supernatant was kept at −35°C until use. Secreted albumin was measured by ELISA as previously described [Mitaka et al., 1995].

Western Blot Analysis

The dishes were washed with PBS and then treated with MatriSperse™ Cell Release Solution (Becton Dickinson) for 15 min at 37°C. Thereafter, 300 μl of buffer solution (10 mM HEPES [pH 7.2], 0.25 M sucrose, 0.5 mM $MgCl_2$) was added to the dish. The cells were scraped and collected into microcentrifuge tubes. After pipetting several times with a microsyringe (Hamilton Com, Reno, NV), homogenates were centrifuged at 500*g* for 5 min at 4°C. The supernatants (microsomal fraction) were kept at −35°C until use. The pellets were resuspended in 50 μl of buffer (20 mM Tris-HCl [pH 7.4], 150 mM NaCl, 0.5% deoxycholate, 1 mM EDTA, 2 mM phenylmethylsulfonic acid, 1% NP-40, 200 KIU/ml aprotinin, 20% glycerol, and 0.4 M KCl) and gently mixed for 30 min at 4°C. After centrifugation at 13,000*g* for 15 min, the supernatant was stored at −35°C (nuclear protein fraction). Concentrations of the protein

were measured using a BCA Protein Assay kit (Pierce, Rockford, IL). Samples (medium: 1 μl/lane; microsomal and nuclear protein fractions: 10 or 20 μg/lane) were separated by SDS–polyacrylamide gel electrophoresis (PAGE) and then transferred electrophoretically to an Immobilon-P membrane (Millipore Corp., Bedford, MA) with a semi-dry transfer cell (BioRad, Richmond, CA). Rabbit anti-albumin, anti-transferrin, anti-α_1-antitrypsin, anti-fibrinogen (Cappel, Costa Mesa, CA), anti-TO (a gift from T. Nakamura), anti-SDH (a gift from R. Kanamoto), anti-C/EBPα, anti-C/EBPβ, goat anti-HNF1α, anti-HNF3α, anti-HNF4α, anti-HNF6, and mouse anti-PCNA antibodies were used. Horseradish peroxidase-conjugated anti-rabbit IgG, anti-goat IgG, and anti-mouse IgG antibodies (DAKO) were applied and positive bands were detected by incubation in Super-Signal West Dura Extended Duration substrate (Pierce). To induce the expression of TO and SDH, the cells were treated with both 10^{-5} M dexamethasone and 10^{-7} M glucagon.

Northern Blot Analysis

Total RNA was extracted from the cells using the single-step thiocyanate–phenol–chloroform extraction method [Chomczynski and Sacchi, 1987] as modified by Xie and Rothblum [1991]. Total RNA (20 μg/lane) was loaded on 1% agarose gel containing 0.5 mg/L of ethidium bromide. Gels were capillary-blotted in 20 × SSPE (3 M NaCl, 173 mM NaH_2PO_4, 25 mM EDTA) onto a nylon membrane (Hybond-N, Amersham) and fixed by ultraviolet light. For the detection of TO and SDH mRNAs, alkaline phosphatase (AP)-labeled cDNA probes were prepared from rat TO cDNA (full 1.7 kb *Eco*RI fragment; a gift from T. Nakamura), rat SDH cDNA (full 1.45 kb *Eco*RI fragment; a gift from R. Kanamoto) using an AlkPhos DIRECT Labeling and Detection System with CDP-Star (Amersham). The method used followed the manufacturer's manual (Amersham).

Perpendicular Sections of Cultured Cells

Perpendicular sections of the colony were examined by using semithin sections of the materials in the process of transmission electron microscopy (TEM). Details of the procedure were previously described [Mitaka et al., 1999].

RESULTS

Morphological Changes of SHs

When hepatic cells, including MHs, SHs, liver epithelial cells (LECs), Kupffer cells, sinusoidal endothelial cells, and stellate cells were cultured in the modified DMEM, SHs rapidly proliferated and formed a colony. Under these culture conditions not only SHs but also LECs and stellate cells proliferated and some SH colonies were gradually surrounded by those cells as previously described [Mitaka et al., 1999]. The colonies not completely surrounded by NPCs continued to expand faster than those surrounded by them and were maintained in a monolayer (Fig. 1A,D). On the other hand, some SHs surrounded and invaded by NPCs gradually changed shape, which looked like rising/piling-up on the colony, and their size became larger (Fig. 1B,E). Their morphology was similar to MHs and they were sometimes binucleate. The piled-up cells formed liver-plate like structures and bile canaliculi (BC) were observed between the cells (Fig. 1C,F).

Immunocytochemistry for LETFs in SH Colonies

Expression of LETFs such as HNF4α, HNF6, and C/EBPα has been reported to be related to hepatic differentiated functions [Cereghini, 1996; Uzma and Costa, 1996]. Therefore, we carried out immunofluorescent staining for LETFs to examine whether LETF expression correlated with the morphological changes of the cells. As shown in Figure 1, HNF4α was expressed in all hepatocytes, including SHs (Fig. 1G). However, neither HNF6 nor C/EBPα was observed in the nuclei of SHs (Fig. 1J,M).

Fig. 1. Expression of HNF4α, HNF6, and C/EBPα proteins in colonies. Triple immunostaining for LETFs (green), E-cadherin (red), and DAPI (blue) shown by digital images analyzed by the CELLScan system. Colonies were classified into three types: those colonies consisting of only SHs and having a flattened shape (flat: A, D, G, J, M); colonies consisting of SHs and large cells (large: B, E, H, K, N); colonies consisting of rising and/or piled-up cells (piled-up: C, F, I, L, O). (A–C) Phase-contrast micrographs of typical colonies of each type are shown. The area indicated by white arrowheads in (B) consists of large, tall cells. The white arrows in (E) show large, binucleate hepatocytes. The area indicated by white arrowheads in (C) shows SHs rising/piled up. The black arrows in (F) show BCs. (D–F) Enlarged photos of the areas surrounded by the squares in (A), (B), and (C), respectively. Scale bars, (A–F), 100 μm. (G–I) Images of cells in each type of colonies for HNF4α. (J–L) Images of cells in each type of colonies for HNF6. (M–O) Images of cells in each type of colonies for C/EBPα. The images are three-dimensionally reconstructed by calculating 30 planes at 0.4-μm intervals. Scale bars, (G–P) 40 μm.

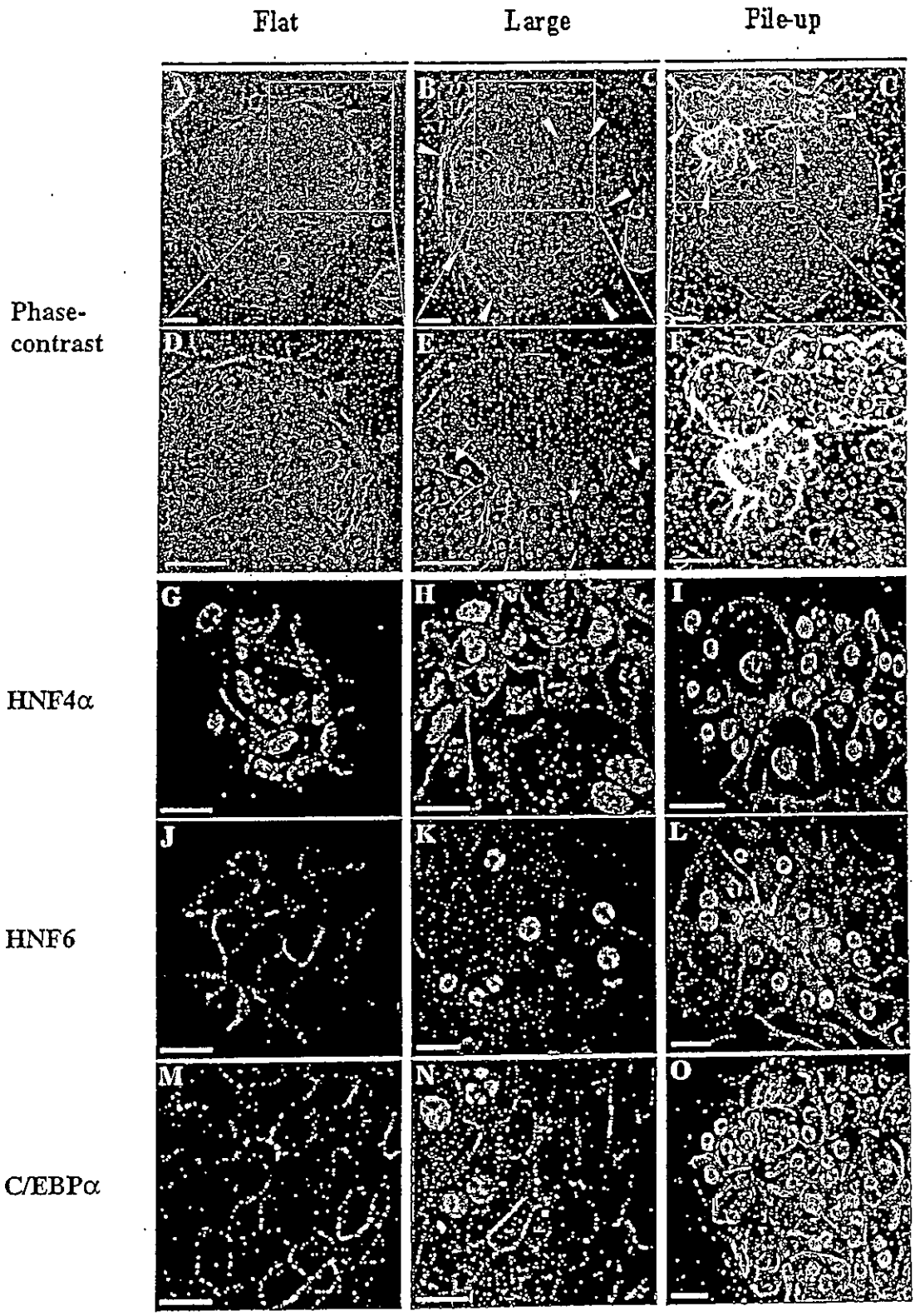
Flat
Large
Pile-up
Phase-contrast
HNF4α
HNF6
C/EBPα
A
B
C
D
E
F
G
H
I
J
K
L
M
N
O

Fig. 1.